Article

Thermal Vacuum Test Campaign of the EIRSAT-1 Engineering Qualification Model

Rachel Dunwoody [1,2,*], **Jack Reilly** [1,2], **David Murphy** [1,2], **Maeve Doyle** [1,2], **Joseph Thompson** [2,3], **Gabriel Finneran** [1,2], **Lána Salmon** [1,2], **Conor O'Toole** [4], **Sai Krishna Reddy Akarapu** [1,2], **Jessica Erkal** [1,2], **Joseph Mangan** [1,2], **Fergal Marshall** [1,2], **Eoghan Somers** [2,3], **Sarah Walsh** [1,2], **Daithí de Faoite** [3], **Mike Hibbett** [5], **David Palma** [6], **Loris Franchi** [6], **Lily Ha** [7], **Lorraine Hanlon** [1,2], **David McKeown** [2,3], **William O'Connor** [2,3], **Alexey Uliyanov** [1,2], **Ronan Wall** [1,2], **Brian Shortt** [8] **and Sheila McBreen** [1,2]

1 School of Physics, University College Dublin, D04 V1W8 Dublin, Ireland; jack.reilly@ucdconnect.ie (J.R.); david.murphy.5@ucdconnect.ie (D.M.); maeve.doyle.1@ucdconnect.ie (M.D.); gabriel.finneran@ucdconnect.ie (G.F.); lana.salmon@ucdconnect.ie (L.S.); sai.akarapu@ucdconnect.ie (S.K.R.A.); jessica.erkal@ucdconnect.ie (J.E.); joseph.mangan@ucdconnect.ie (J.M.); fergal.marshall@ucdconnect.ie (F.M.); sarah.walsh.2@ucdconnect.ie (S.W.); lorraine.hanlon@ucd.ie (L.H.); alexey.uliyanov@ucd.ie (A.U.); ronan.wall@ucd.ie (R.W.); sheila.mcbreen@ucd.ie (S.M.)
2 Centre for Space Research, University College Dublin, D04 V1W8 Dublin, Ireland; joseph.thompson@ucdconnect.ie (J.T.); eoghan.somers@ucdconnect.ie (E.S.); david.mckeown@ucd.ie (D.M.); william.oconnor@ucd.ie (W.O.)
3 School of Mechanical and Materials Engineering, University College Dublin, D04 V1W8 Dublin, Ireland; daithi.defaoite@ucd.ie
4 School of Mathematics and Statistics, University College Dublin, D04 V1W8 Dublin, Ireland; conor.o-toole.1@ucdconnect.ie
5 Irish Manufacturing Research, D24 WCO4 Dublin, Ireland; mike.hibbett@gmail.com
6 Redu Space Services for European Space Agency, European Space Security and Education Centre (ESEC), 6890 Libin, Belgium; david.palma@ext.esa.int (D.P.); loris.franchi@ext.esa.int (L.F.)
7 HE Space Operations for European Space Agency, European Space Research and Technology Centre (ESTEC), 2201 Noordwijk, The Netherlands; lily.ha@ext.esa.int
8 European Space Agency, European Space Research and Technology Centre (ESTEC), 2201 Noordwijk, The Netherlands; brian.shortt@esa.int
* Correspondence: rachel.dunwoody@ucdconnect.ie

Abstract: CubeSats facilitate rapid development and deployment of missions for educational, technology demonstration, and scientific purposes. However, they are subject to a high failure rate, with a leading cause being the lack of system-level verification. The Educational Irish Research Satellite (EIRSAT-1) is a CubeSat mission under development in the European Space Agency's (ESA) Fly Your Satellite! Programme. EIRSAT-1 is a 2U CubeSat with three novel payloads and a bespoke antenna deployment module, which all contribute to the complexity of the project. To increase the likelihood of mission success, a prototype model philosophy is being employed, where both an engineering qualification model (EQM) and a flight model of EIRSAT-1 are being built. Following the assembly of the EQM, the spacecraft underwent a successful full functional test and month-long mission test. An environmental test campaign in ESA Education Office's CubeSat Support Facility was then conducted with the EQM where both vibration and thermal verification test campaigns were performed. The focus of this paper is the thermal testing and verification of the EIRSAT-1 EQM. Over three weeks, the EQM was subjected to one non-operational cycle, three and a half operational cycles, and a thermal balance test in a thermal vacuum chamber. After dwelling at each temperature extreme, functional tests were performed to investigate the performance of the spacecraft in this space representative environment. The approach to planning and executing the thermal testing is described in detail including the documentation required, set up of the test equipment, and determination of the test levels. Overall, the campaign demonstrated that the mission can successfully operate in a space environment similar to that expected in orbit, despite encountering a number of issues. These issues included a payload displaying anomalous behaviour at cold temperatures and needing to redefine test levels due to an insufficient understanding of the internal dissipation in the spacecraft. A total of two major and three minor non-conformances were raised. Crucially, these issues could not have been

found without thermal testing, despite the comprehensive ambient tests performed. The main results and lessons learned during this thermal test campaign are presented with the aim of guiding future missions on optimal approaches in organising and executing the thermal testing of their CubeSats.

1. Introduction

CubeSats are small-scale satellites defined in standard units [1], where typically one unit, a 1U, is a 10 cm × 10 cm × 10 cm cube of mass less than 1.33 kg [2]. They were initially developed as an educational tool to provide university students with the opportunity to experience the full life cycle of a space mission [3,4] as they have relatively short project timelines and are low cost when compared to large space missions [5,6]. Over 1000 CubeSats have been launched since the standard was first proposed [7]. In a short period of time, their popularity has grown exponentially as it has been realised they could be harnessed for space science, space weather, and technology demonstration purposes [8–11]. This small-scale satellite standardisation has facilitated the establishment of commercial off-the-shelf (COTS) components which contributes to reduced development timescales, reduced cost, and more emphasis on the scientific goals of the mission [12]. However, of the first one hundred CubeSat missions launched, those developed by university teams had a high failure rate of nearly 50% [13,14]. Many projects failed due to a lack of meticulous system-level testing [15–17].

The Educational Irish Research Satellite, EIRSAT-1, is a 2U CubeSat being designed, built, and tested by a student-led team in University College Dublin (UCD) [18]. EIRSAT-1 was selected for the second edition of the European Space Agency (ESA) Education Office's Fly Your Satellite! (FYS!) Programme [19]. The main subsystems of this mission are displayed in Figure 1. This 2U CubeSat mission has educational, scientific, and technology demonstration objectives. The educational aims include skills development and outreach. The scientific and technology development objectives are supported by the three experimental subsystems on board: the Gamma-ray Module (GMOD), ENBIO Module (EMOD), and Wave Based Control (WBC). In addition, the spacecraft TMTC antenna was designed and built in-house. The three payloads and the custom antenna make EIRSAT-1 a complex mission.

Figure 2 summarises the mission objectives of the EIRSAT-1 project based on its three payloads. GMOD is a bespoke gamma-ray detector [20,21] constructed based on heritage instrument development [22,23] and its firmware has been developed in-house [24]. GMOD will observe gamma-ray bursts (GRBs), the most luminous electromagnetic explosions in the universe known to involve the birth of a black hole [25]. GMOD comprises a scintillator coupled to silicon photomultipiers read out by a custom application specific integrated circuit (ASIC) and motherboard (MB) [26,27] and is located in the upper half of the stack, as shown in Figure 1. EMOD is a thermal surface treatment experiment where the on-orbit performance of ENBIO Ltd.'s thermal coatings, similar to those currently on ESA's Solar Orbiter mission [28], will be monitored throughout the mission. Resistance temperature detectors (RTDs) are mounted on the back of four thermal coupons at the top of the stack, two treated with SolarBlack and two treated with SolarWhite [18]. WBC is a software payload which will provide the first in-flight test of a novel attitude control algorithm [29,30]. The electrical power subsystem (EPS), attitude determination and control system (ADCS), CMC transceiver, and on-board computer (OBC) of EIRSAT-1 are all COTS components from AAC Clyde Space. The EIRSAT-1 communications subsystem makes use of an in-house developed antenna deployment module (ADM) [31]. The ADM contains four coiled antenna elements, each attached to a door that is held closed by two tensioned meltlines for redundancy. The deployment of the antenna is performed by passing current

through one of two burn resistors which are in contact with the lines. The ADM can been seen at the bottom of the stack in Figure 1. The OBC software has been adapted to interface with the in-house developed software and firmware for each of the on-board experiments [32].
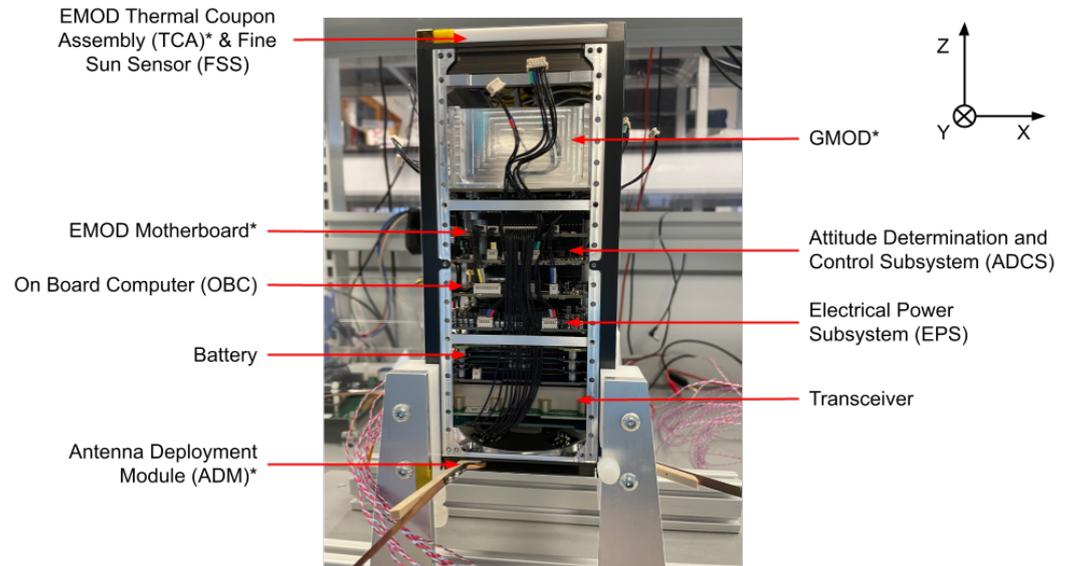
Figure 1. EIRSAT-1 EQM with internal components visible, as the image was taken during EQM assembly before the solar panel and structural shear panel were installed. The components marked with an asterisk (*) are components developed in-house and the remaining subsystems are commercial, off-the-shelf components.
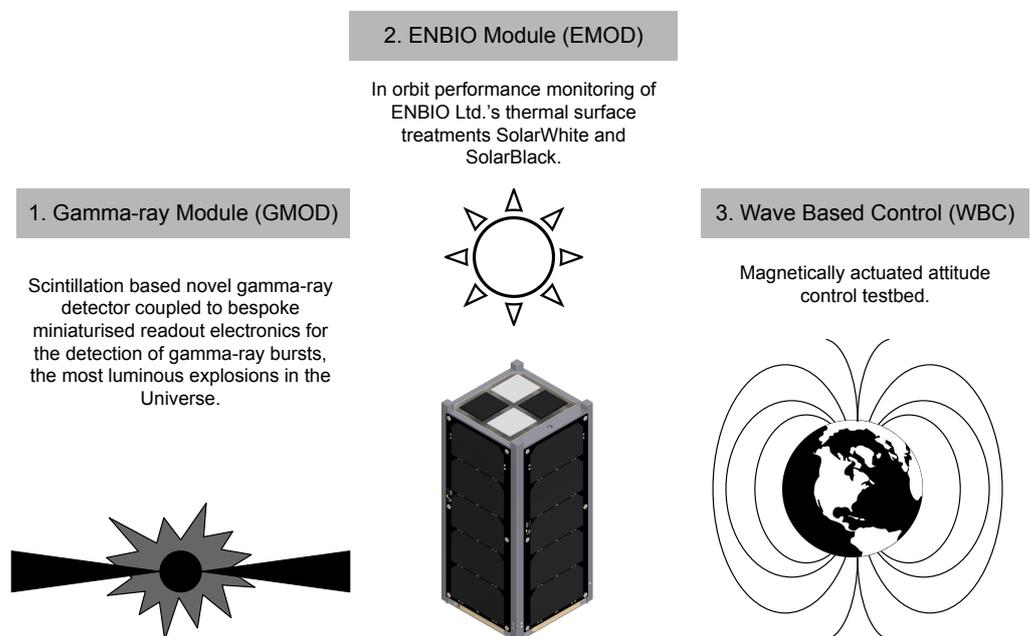
Figure 2. Overview of mission objectives. GMOD is a bespoke gamma-ray instrument that will detect GRBs. EMOD will monitor the performance of ENBIO Ltd.'s thermal surface treatments. The mission will also provide the first in-orbit test of WBC, a novel attitude control algorithm.

There are a variety of risk reduction strategies employed in CubeSat projects, such as risk response matrix (RRM), fault tree analysis (FTA) and failure mode and effects analysis (FMEA) (e.g., [33–35]). The EIRSAT-1 project maintains a risk register and executes fault

detection, isolation, and recovery (FDIR) methods during the EIRSAT-1 software development [32]. The main aspects of the EIRSAT-1 risk management plan are the implementation of a prototype model philosophy—where both an engineering qualification model (EQM) and a flight model (FM) of the spacecraft (S/C) are being developed [36]—and extensive test campaigns. The EQM has been more rigorously tested to qualification levels and durations to verify the design for space flight. A full functional test (FFT) [36,37], mission test (MT) [38], and environmental test campaign (ETC) have been performed on the EQM. The FM will be tested to lower acceptance levels and durations, launched, and operated in space. As part of the ESA FYS! Programme, expertise and state-of-the-art facilities have been provided by ESA to qualify the mission for space flight, further increasing the robustness. Several test campaigns, at both subsystem [39] and system levels, must be completed, following the European Cooperation for Space Standardisation (ECSS) [40] and FYS! standards, to qualify the mission.

The ETC of EIRSAT-1 consists of two main components: vibration testing and thermal testing. Vibration testing is conducted to ensure the spacecraft will remain functional after the violent vibrations it will experience during launch [41]. Thermal testing is performed to determine the behaviour of the satellite in vacuum conditions at its temperature extremes [42]. This paper will focus on the thermal tests performed on the EQM of EIRSAT-1 at the ESA CubeSat Support Facility (CSF) in Belgium [43] . According to ECSS, the thermal testing and verification campaign for a satellite has three components [44]:

- Thermal Vacuum Test: To demonstrate that the system functions fully in the expected operational extremes the mission will be exposed to in orbit [42].
- Thermal Cycle Test: To verify the test item design and reveal workmanship errors through stressing the item under test (IUT).
- Thermal Balance Test: To obtain data of the spacecraft in different operational scenarios at temperature extremes to compare to the simulated thermal model, discussed in Section 2.2. Adjustments can then be made to the thermal model such that it is a better representative of the spacecraft and its thermal control system [45].

The thermal vacuum and thermal cycling tests are performed in parallel and the ECSS standard recommends one non-operational cycle and three operational cycles with dwell phases with a stabilisation criterion of <1 K/h for the thermal vacuum cycling test [44]. The final aspect of the thermal testing campaign is the thermal balance (TBal) test. During the TBal test, all the temperature sensors of the S/C must reach a state where a specified stabilisation criterion is met, with a typical criterion being $\sim{<}0.5$ K/5h. This test campaign also facilitates extensive testing of the ground based interface with the S/C e.g., data acquisition and visualisation. In the event of anomalies, investigations must be completed via the ground station interface to the S/C [46,47] and the mission must be recovered in a more realistic scenario, where the CubeSat can not be physically observed.

During the EIRSAT-1 EQM thermal testing and verification campaign, a thermal vacuum test, thermal cycle test, and a thermal balance test was performed over three weeks at the ESA Education's CSF from the 27 September 2021 to 14 October 2021. Section 2 details the activities and documentation that was required to be completed in preparation for the EQM thermal test campaign. The set-up of the test item in the thermal vacuum (TVAC) chamber at the CSF and the required ground support equipment for the functional testing is presented in Section 3. The execution of the EQM thermal test campaign, the major results and anomalies encountered are discussed in Section 4. The lessons learned by the EIRSAT-1 team while preparing and completing the thermal testing and verification campaign, are presented in Section 5 and will be beneficial to the CubeSat community in qualifying their missions for spaceflight. Finally, the plan for future work is given in Section 6.

2. EIRSAT-1 Thermal Vacuum Test Campaign Preparation

The thermal vacuum cycling and thermal balance phase tests are part of the full suite of tests that are required to qualify a spacecraft for launch and operation in space. Figure 3

presents the EIRSAT-1 EQM thermal test campaign in the context of the other necessary test activities. The ETC could not commence until both the FFT [36,37] and MT [38] of the EQM were completed. Modified versions of the FFTs were combined into scripted suites of testing called reduced functional test (RFT) and very reduced functional test (VRFT) to test the spacecraft at various points of the thermal test campaign, as described briefly in Table 1.
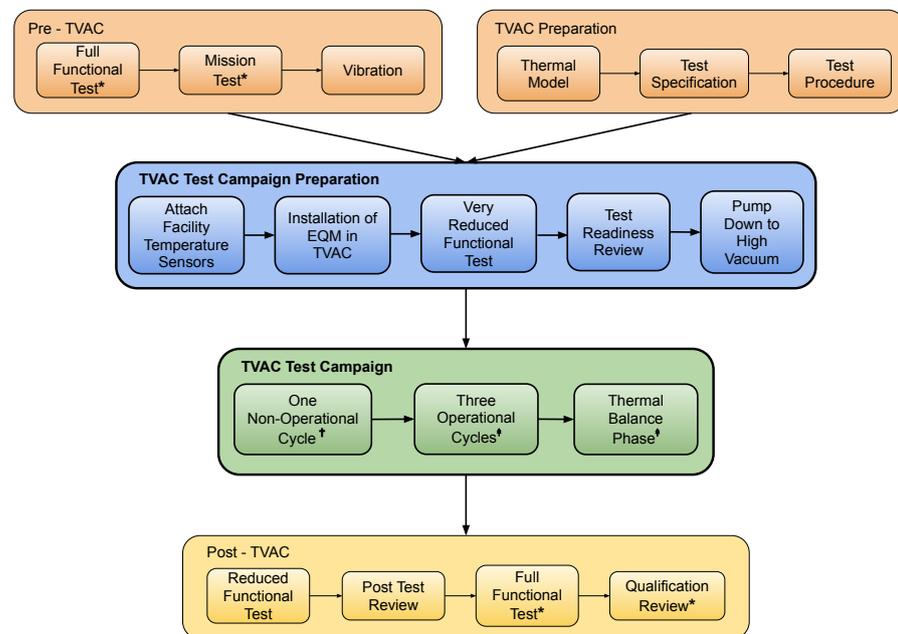
*Location of testing: University College Dublin
†Switch On Test performed during each Non-Op Dwell (one hot and one cold)
♦VRFT performed during each Op Dwell and after each TB phase

Figure 3. Overview of the activities before, during, and after the thermal testing campaign.

Table 1. Overview of functional tests performed with EQM before, during, and after the thermal test campaign.

Test Activity	Description
FFT	The full functional test fully assesses the performance of the system and also verifies functional requirements.
RFT	The reduced functional test focuses on mission-crucial hardware functions and includes a subset of tests performed in the FFT to verify the performance of the spacecraft after environmental tests.
VRFT	The very reduced functional test contains a subset of the tests in the RFT; the selection criteria was that the test could be completed while the satellite was installed in the thermal vacuum chamber.

2.1. Required Documentation

As part of the FYS! Programme, detailed documentation of the plan for each test campaign must be completed. The following are the set of documents, tailored from the ECSS standard by ESA [44], that need to be submitted before, during, and after a test campaign.

- Test Specification (TSpe): The thermal testing campaign TSpe details the proposed test equipment configuration, thermal cycling and balance agenda, test schedule, requirements verified, functional tests, and pass/fail criteria for the test campaign. The TSpe was examined by an ESA thermal expert. The information and advice received from ESA was crucial to the success of the campaign.

- Test Procedure (TPro): The TPro contains a detailed step-by-step description of all of the activities in the test campaign and is derived from the TSpe. During testing, these step-by-step documents are filled out to form the As-Run Procedure.
- Test Readiness Review (TRR): The TRR is completed directly before the test activity is started to verify that all conditions to start the test have been met. During the TRR, it was ensured that all relevant documentation (TSpe, TPro) was approved and available, the test facility was prepared, the IUT was appropriately configured and the ground support equipment (GSE) was assembled and connected correctly.
- Post Test Review (PTR): At the end of the test campaign, a PTR is performed to formally end the test campaign and confirm that the tests had been performed according to the TPro, any deviations have been recorded, the objectives have been achieved, and all data has been archived. The actions that must be completed by the team are also indicated, including the submission of any non-conformance reports (NCRs) and the test report (TRPT), which are described in the following points.
- Test Report (TRPT): The TRPT is completed after the test campaign, it describes the test execution, the main results of the campaign, and any anomalies that were observed. The As-Run Procedure is appended to the end of this report as a record of all the activities followed during the test campaign.
- Non-Conformance Report (NCR): An NCR is a document recounting the occurrence of any anomalies observed during the test campaign and the investigation that followed to determine the root cause of the non-conformance and, when applicable, the solution to the encountered issue. Both minor and major NCRs were raised during the thermal test campaign. An example of a minor NCR is presented in Section 4.2.1 and a major NCR is discussed in Section 4.2.2.

All of these documents must be completed for the qualification acceptance board, which is held to review all the test results and conclude on the success of the test campaign in achieving its objectives. In the case of the EIRSAT-1 EQM, the review board is to conclude if the CubeSat design has been qualified for spaceflight based on the results of the FFTs, MT and ETC. The subsequent sections will detail the EIRSAT-1 EQM thermal test campaign, comparing the test plan laid out in the test specification to the actual execution of the test as in the TRPT, with a summary of the major lessons learned in Section 5.

2.2. Test Levels

An understanding of the thermal properties of the system is required when planning the thermal test campaign [48]. A challenge to performing a realistic thermal test campaign of an S/C is accurately representing the space environment and heat transfer processes the mission will experience [49]. Satellites must be capable of operating in a vacuum environment and will experience extreme temperatures during the mission lifetime, with periods in direct sunlight and in eclipse behind the Earth. Due to the lack of atmosphere, the primary method of heat transfer between the satellite and its environment is radiation. There will also be heat transfer between components of the satellite via conduction and radiation [50]. As CubeSats are relatively small, the thermal properties of the system can be significantly impacted by the heat generated by the electronic components e.g., CMC board when transmitting. All of these aspects must be considered in the planning and execution of a thermal testing and verification campaign. In the case of EIRSAT-1, it was important to take into consideration the active thermal control process in the battery which has three heaters which turn on when the battery is cold ($\sim$<0 °C). Passive thermal control elements in the S/C include the spacers between printed circuit boards (PCBs) in the stack and the multi layered insulation blanket under the EMOD thermal coupons to thermally isolate it.

During environmental testing of EIRSAT-1 EQM, the satellite was subjected to a number of thermal cycles, simulating the thermal stress that EIRSAT-1 will endure during orbit around Earth. A major aspect of the preparation for this test campaign was to determine the test levels the S/C needed to be cycled through to ensure it will operate in orbit. Initially,

the operational and non-operational temperature limits of all the components of EIRSAT-1 were determined, as presented in Table 2, using the manufacturer specifications.

Table 2. Operational and non-operational limits of components and subsystems.

Item	Operational		Non-Operational	
	Min (°C)	Max (°C)	Min (°C)	Max (°C)
SiPM	−45	+85	−45	+85
GMOD CPLD	−40	+85	−40	+105
GMOD Microcontroller	−40	+85	−40	+105
EMOD Microcontroller	−40	+85	−40	+105
OBC	−40	+80	−40	+85
ADCS Motherboard	−40	+80	−40	+85
EPS	−40	+85	−50	+100
Comms	−25	+61	−40	+85
Battery	−10	+50	−20	+60
Solar Arrays	−40	+80	−40	+85
Fine Sun Sensor	−30	+85	−30	+85

The overall temperature profile of the TVAC must be broadly representative of the space environment while not allowing components or subsystems to become too hot or cold, in both non-operational and operational modes. The thermal analysis that was performed with EIRSAT-1, for an earlier phase of the FYS! Programme called Critical Design Review, using the C&R Thermal Desktop tool suite [51] was used to help determine the temperature test levels.

In this thermal analysis, the satellite's thermal response was modelled for approximately ten orbits, with orbital parameters similar to the International Space Station (ISS), as presented in Table 3. Ten orbits were simulated to allow the satellite component's temperatures to stabilise and oscillate around a more realistic mean temperature. Thermal Desktop allowed for the performance of Finite Element Analysis, breaking up the relatively complex geometries in the S/C into a large collection of basic shapes. A number of environmental sources of radiation were included such as solar flux, reflected solar flux due to the Earth's albedo and infrared radiation re-emitted by the planet.

Table 3. Orbital parameters used for EIRSAT-1 during thermal analysis.

Orbital Parameter	EIRSAT-1 Value
Orbital Inclination (°)	51.6
Right Ascension of Ascending Node(°)	315.8
Argument of Periapsis (°)	273.4
Eccentricity	0.001
Altitude at Apogee (km)	412.64

The response of the spacecraft was simulated in different low earth orbit (LEO) scenarios, typical of CubeSat missions, including operational and non-operational modes in nominal, cold, and solstice cases. The simulation results indicated that when a modelling uncertainty of ±10 °C was included, none of the components were found to exceed their operational or non-operational limits in any of the simulated scenarios. The component with the most constrained temperature limits could be used to define the maximum and minimum temperature limits for the thermal cycle. It was concluded that the EQM thermal test levels should be limited by the battery which, as shown in Table 2, has the smallest operational and non-operational temperature ranges.

As part of determining the test levels for the TVAC campaign, a temperature reference point (TRP) must be defined. A TRP is a physical point defined on the S/C structure equipped with a temperature sensor that serves as a thermal interface between the CubeSat

and the test facility apparatus [52]. The TRP should be representative of the average temperature of the CubeSat and the offset between the temperature of the TRP and other components can be estimated from the thermal analysis performed. The location of the TRP of EIRSAT-1 was at the centre of the +Y face of the +X, +Y corner rail. The temperature at this point was measured using a T Type thermocouple. For redundancy, a second sensor was installed on the +Y face of the −X, +Y corner rail as a back up to the TRP (BKTRP). These locations, on the structure of the S/C, were selected as they allow for the most rapid response between the chamber settings and the IUT, reducing the risk of any temperature limits being exceeded and protecting the health of the spacecraft's temperature-sensitive subsystems.

The final proposed test levels in the test specification were determined by taking into account the limits of the battery and the expected gradient between the TRP and the internal components as calculated in the thermal analysis. The difference in the operational and non-operational test levels is due to the fact that when the satellite is operational the internal components dissipate heat to the system.

$T_{max, non-op}$ was defined as +56 °C to stress all the components while taking into account that the battery has a non-operational limit of 60 °C and allowing for a test level tolerance of −0/+4 °C. Based on the model, the EIRSAT-1 battery is ~9.5 °C warmer than the structure when the spacecraft is powered on and transmitting over radio frequencies (RF). In the hot operational case, the maximum temperature the battery can be at is 50 °C, and taking the case when RF is on and accounting for a tolerance of −0/+4 °C, $T_{max, op}$ is defined as +36.5 °C.

For the operational and non-operational cold cases, though the battery does have heaters that turn on at ~0 °C, it was decided not to bring the battery temperature below −10 °C when ON and below −20 °C when OFF to protect the subsystem. $T_{min, non-op}$ and $T_{min, op}$ were defined as −16 °C and −6 °C, respectively, based on the limits imposed by the battery and accounting for the test level tolerance of −4/+0 °C.

An initial cold stress phase was added in the cold cycles to stress the external components (fine sun sensor (FSS), EMOD, solar arrays, ADM, and the structure) of the EQM without allowing the internal components to exceed their operational limits. The FSS is the limiting case with a limit of −30 °C, so the $T_{min, stress}$ was defined as −26 °C. Since the internal components will cool at a slower rate, a conservative ~1 h dwell at $T_{min, stress}$ was proposed to avoid approaching the operational limits of the battery during the stress phase.

For the TBal test levels, an extra 5 °C margin was added to the $T_{max, op}$ and $T_{min, op}$ test levels as it was an unnecessary risk to bring the subsystems close to their operational limits. The $T_{max, TBal}$ was defined as +31.5 °C and $T_{min, TBal}$ as −1 °C, including the test level tolerance of −0/+4 °C and −4/+0 °C, respectively. Table 4 presents the proposed test temperature levels, discussed above, for the system in non-operational, operational, and TBal conditions. The final column indicates the operator set points accounting for the test equipment being accurate to within 1 degree.

Table 4. Test plan operational, non-operational, and thermal balance temperatures.

Test Level	Temperature (°C)	Tolerance (°C)	TRP Range (°C)
$T_{max, non-op}$	+56	−0/+4	+57 to +59
$T_{min, non-op}$	−16	−4/+0	−17 to −19
$T_{max, op}$	+36.5	−0/+4	+37.5 to 39.5
$T_{min, op}$	−6	−4/+0	−7 to −9
$T_{min, stress}$	−26	−4/+0	−27 to −29
$T_{max, TBal}$	+31.5	−0/+4	+32.5 to 34.5
$T_{min, TBal}$	−1	−4/+0	−2 to −4

Table 5 presents the remaining test levels that were defined as part of the test specification . The thermal analysis revealed temperature gradients that were higher than could be

produced with the radiation-based test set-up in the CSF TVAC, so a temperature gradient of 0.1 °C/min was defined. This gradient was based on other CubeSat TVAC campaigns performed at the CSF. A dwell time of two hours was proposed for the dwells at $T_{max,\ non\text{-}op}$, $T_{max,\ op}$, $T_{min,\ non\text{-}op}$ and $T_{min,\ op}$ to allow all the components of the satellite to reach the desired temperature extremes for qualification. Only a one-hour dwell was proposed for the $T_{min,\ stress}$ to ensure that the internal components did not approach their temperature limits while still stressing the external components at a lower temperature.

Table 5. Gradient, dwell, and TBal values proposed in the test specification.

Parameter	Values
Temperature Gradient Range	0.1 °C/min
Dwell Time	120 min
Stress Dwell Time	~60 min
TBal Stabilisation	0.5 K/4 h

2.3. Test Plan

The test plan profile of the operational and non-operational cycles and thermal balance phases of the EQM is presented in Figure 4.
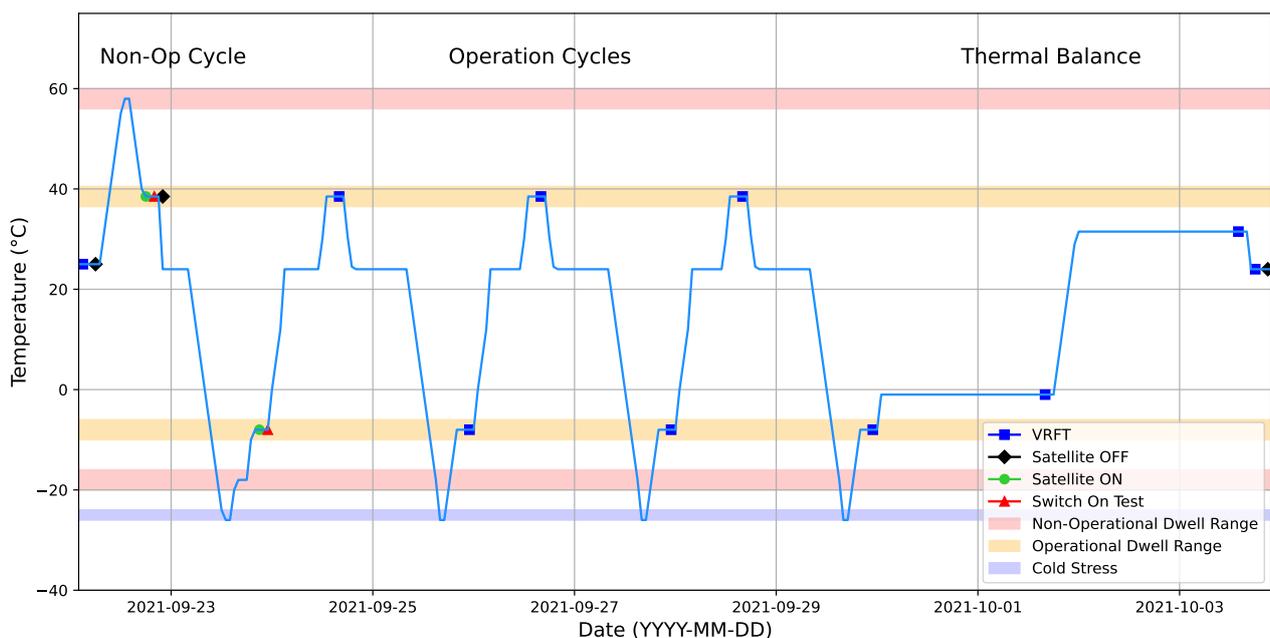
Figure 4. Planned thermal profile (non-operational cycle, three operational cycles, TBal) and test activities (switch on tests, VRFTs) as included in the thermal testing TSpe and TPro.

Initially, the S/C was to be subjected to a non-operational cycle, including a cold stress, from +56 °C to −26 °C. Three operational cycles, including cold stress phases, were then to be performed between −26 °C and +36.5 °C. Finally, two thermal balance phases at +31.5 °C and −1 °C were planned. These phases have much longer temperature plateaus to allow for the stabilisation criterion of 0.5 K/4 h to be achieved. In Figure 4, the green circles indicate the spacecraft being turned on and the black diamonds indicate the spacecraft being switched off. The red triangles indicate a switch on test and the blue squares indicate a VRFT being performed which are both described in Section 2.4. Each functional test was to be performed after the 2 h dwell at either the hot or cold operational extreme temperatures.

2.4. Functional Test Description

Three types of functional tests were performed during the EIRSAT-1 EQM thermal test campaign to verify performance: switch on test, VRFT, and RFT. Table 6 gives an overview of some of the test suites which are covered in more detail below.

The most basic functional test was the switch on test, performed once all subsystems reached operational temperature limits, after dwelling at non-operational extremes. The EQM was turned on, the subsystem power on test, as described in Table 6 was performed and then the EQM was powered off.

Table 6. Description of the tests included in the RFT and VRFTs during thermal testing. Entries marked with an asterisk (*) were performed as part of the VRFT.

Test Name	Test Description
ADM Primary Deployment Burn *	Primary resistors in ADM are burned, and successfully deploy the four antennas unless antennas have already been released.
ADM Secondary Deployment Burn *	Secondary resistors in ADM are burned, and successfully deploy the four antennas unless antennas have already been released.
Subsystem Power On *	To confirm all essential loads (EPS, BAT, CMC, ADCS, and OBC) are turned on upon power ON of the spacecraft, a telecommand (TC) is sent to the S/C to obtain the version parameter of each subsystem.
RBF Inhibit Insertion	Confirms the SC powers off and charging takes place when RBF pin is inserted and the SC powers on when RBF pin removed.
Inhibits Insertion	Ensures that the spacecraft does not power on when any one of the inhibits are activated.
DTMF Reset	Verifies that the receipt of the correct DTMF tones by the spacecraft resets the OBC.
Uplink/Downlink *	Verifies that a packet can be sent and received between the spacecraft and the ground station.
Beacon stop/start	Verifies that the beacon is transmitted once a minute and RF can be stopped upon command from GS.
ADCS On-board Sensors	ADCS bus voltages and currents checked. On-board magnetometers and rate gyroscopes are excited to check noise, polarity, and correct function.
ADCS External Sensors	Five coarse sun sensors and one fine sun sensor are all excited using a torch (Fenix LD22) to test functionality.
ADCS Magnetorquers (MTQs) *	Functionality confirmed by driving each coil at duty cycles of 100% in both directions for 20 s each.
OBC Reduced Mode Changes *	Verifies that the OBC can transition between different operational modes. Reduced as no transitions to/from WBC mode were made.
Temperature Sensors *	Read all temperature sensors (BAT, EPS, ADCS, magnetometers, gyro, CMC).
GMOD Functional *	Payload is power cycled to confirm configuration is correct after power on. GMOD experiment set up to stream data to the OBC to generate a spectrum and lightcurve using 2% thoriated rods as a gamma-ray source.
EMOD Functional *	Payload is power cycled to confirm configuration is correct after power on. EMOD experiment is set up to stream RTD readings to OBC.

The most extensive set of testing was the RFT. The RFT was performed after the test campaign, with the S/C in ambient conditions on a test bench after being uninstalled from the TVAC. All of the functional tests described in Table 6 were performed during the RFT

to verify the functionality of the payloads and COTS subsystems. Section 4.3 summarises the main results from this functional test.

In Table 6, entries marked with an asterisk (*) were performed as part of the VRFT. The initial VRFT was performed in ambient conditions prior to pump down to high vacuum to ensure the set-up was configured correctly. The results of this VRFT also provided a baseline for comparison with the results of all the VRFTs performed in operational extremes during thermal cycling. The remaining VRFTs were performed after dwelling at each operational hot and cold temperature and after the hot and cold TBal phases. The remove before flight (RBF) inhibit and other power inhibit insertion tests could not be performed during the VRFT as the switches could not be accessed while the satellite was installed in the chamber. Similarly, there was no light source to excite the sun sensors (ADCS external sensors) or way to rotate the satellite to test the functionality of the ADCS on-board sensors. The dual-tone multi-frequency (DTMF) reset and beacon stop/start test were omitted due to time constraints and these had been extensively tested during the EQM FFT and MT campaigns. The details of the individual VRFTs, the results, and the anomalies encountered are presented in Section 4.2.

3. EQM Thermal Test Equipment Set Up

The thermal test set-up consisted of four major elements: the EIRSAT-1 EQM configured for thermal testing (IUT), the test facility consisting of the TVAC chamber and instrumentation system, mechanical ground support equipment (MGSE) required to mount the IUT in the chamber, and electrical ground support equipment (EGSE) to provide power and communicate with the IUT during the test. Each of these elements is described in more detail in the following sections.

### 3.1. EIRSAT-1 EQM Thermal Test Configuration

The satellite was in a test-specific configuration before it was installed in the chamber. The main differences between this configuration and the flight configuration were modifications made to the communications subsystem. In the test configuration, the coaxial cables which connect the transceiver to the ADM were replaced with cables which were passed from the interior of the satellite through a slot in one of the side panels to the chamber flange. On the chamber exterior, these coaxial lines were connected to EGSE including RF attenuators and a software defined radio using GNU Radio [53]. The radio was connected to a computer which ran EIRSAT-1's mission control software and communicated with the satellite over RF. This modification made it possible to test both uplink and downlink using the transceiver in the chamber which would not have been possible while connected to the ADM due to the poor RF environment that the metal shroud of the chamber would provide.

The ADM has two long and two short copper–beryllium tape spring elements which are coiled inside the satellite when stowed and straightened once deployed. The distance between the ends of the longer elements of the ADM is over 1.2 m when deployed. As there was insufficient space inside the chamber for the long antenna elements to deploy without touching the shroud, the longer elements were taped once stowed, such that the doors withholding the elements could open but the elements would not be able to uncoil completely. The thermal model did not include the deployed or stowed antenna element configuration as simplifications were required due to limited resources. Inevitably, the stowing of the elements does marginally change the thermal properties of the system but it was negligible due to their high conductivity. This configuration was selected as it prevented heat transfer via conduction which could have occurred had the antenna elements come into contact with the shroud of the chamber.

3.2. TVAC Chamber and Instrumentation

For the test a cylindrical vacuum chamber with inside diameter 0.6 m and length 0.7 m was used. The chamber is capable of producing a vacuum of 10^{-6} mbar. A thermal shroud, with a temperature uniformity specification of 2 °C, is mounted inside the chamber

which has a controllable temperature between $-60\,°C$ and $+100\,°C$. This shroud completely surrounds the test item with a nearly uniform temperature in all directions. The IUT was suspended from a telescopic rail at the top of the chamber, as in Figure 5, to minimise conduction and make the primary mode of heat transfer radiation between the IUT and shroud, approximating as closely as possible the space environment. This is particularly important for the thermal balance phases.
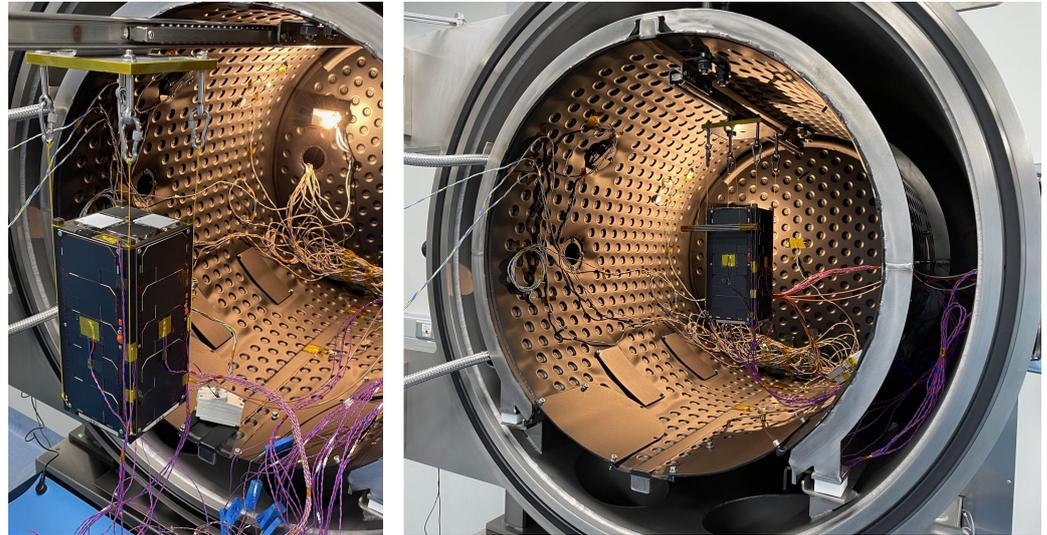
Figure 5. Left: Suspended EIRSAT-1 EQM during installation into CSF TVAC. **Right**: EQM installed in TVAC with 2% thoriated radioactive rods installed in front of satellite to test the GMOD instrument.

Several T Type thermocouples, provided and installed by ESA CSF operators, were attached to the exterior of the spacecraft to measure the response of the satellite to changes in the chamber temperature. The locations of these thermocouples were as follows: ADM outer cover, ADM baseplate, $-X +Y$ corner rail, $+X +Y$ corner rail (TRP), solar cell mass models ($+Y$, $-Y$, $+X$), $-X$ solar panel PCB, FSS housing, and GPS antenna. There were also 14 thermocouples installed internally in the S/C prior to EQM assembly. The number and location of the temperature sensors were selected to monitor the critical components of the subsystems—EMOD thermal coupon assembly, GMOD detector, GMOD MB, EMOD MB, ADCS, OBC processor, battery (top), battery (bottom), CMC, ADM PCB, solar array interior ($+Y$, $-Y$, $+X$, $-X$). All of these thermocouples were routed to the CSF data acquisition system via the TVAC chamber flange. The instrumentation system is capable of logging the temperatures of all thermocouples for the duration of the test with an uncertainty of $\pm 1\,°C$.

3.3. Mechanical Ground Support Equipment

The MGSE mounted on the CSF TVAC chamber's telescopic rail included an aluminium mounting bracket, four stainless steel eye bolts, four carabiners, and eight suspension lines. Prior to installation of the MGSE in the chamber, it was baked out in a vacuum oven to minimise the risk of contamination due to outgassing. The mounting bracket was bolted to the telescopic rail. The four eye bolts were then threaded through the mounting bracket and secured in place using a jam nut. A stainless steel carabiner with a captive locking mechanism was hooked onto each of the eye bolts.

Ultra-high molecular weight polyethylene (dyneema) suspension lines which were securely looped around the corner rail extensions of the satellite were hooked onto the carabiners as the spacecraft was installed in the chamber. The satellite was installed such that the *z*-axis pointed directly up towards the mounting bracket and the *x*-axis pointed out of the chamber door. Two of these lines were attached at each corner of the satellite to ensure there was redundancy in the case of a line failure. Previous verification of this suspension system demonstrated that a single suspension line was enough to take the weight of the

satellite; however, having two lines on each corner ensured that the orientation of the spacecraft would not change. Adjusting the position of the eye bolts and jam nuts allowed for leveling of the satellite and ensured tension was even in the suspension lines.

To improve the similarity between the thermo-optical properties of the test set-up and the space environment, black kapton was applied to the face of the aluminium bracket which would be directly above EIRSAT-1 and to the aluminium solar cell mass models. Solar cell mass models are used for the EQM to reduce project cost [37]. A set of 2% thoriated tungsten rods were also suspended in the TVAC chamber using dyneema parallel to GMOD in the stack as these were the source of gamma radiation used to functionally test GMOD.

3.4. Electrical Ground Support Equipment

A schematic of the end-to-end connections from the EIRSAT-1 spacecraft to the EGSE is presented in Figure 6. The EIRSAT-1 umbilical harness connects to the two EGSE ports located on the −X face of the spacecraft, a 3-pin DF13 RBF socket, which can be used to activate one of the electrical power system inhibits, and a 51-pin nano D umbilical port which allows for full communication between the on board computer and any EGSE, access to the spacecraft's data buses and power lines, and the ability to charge the spacecraft battery.
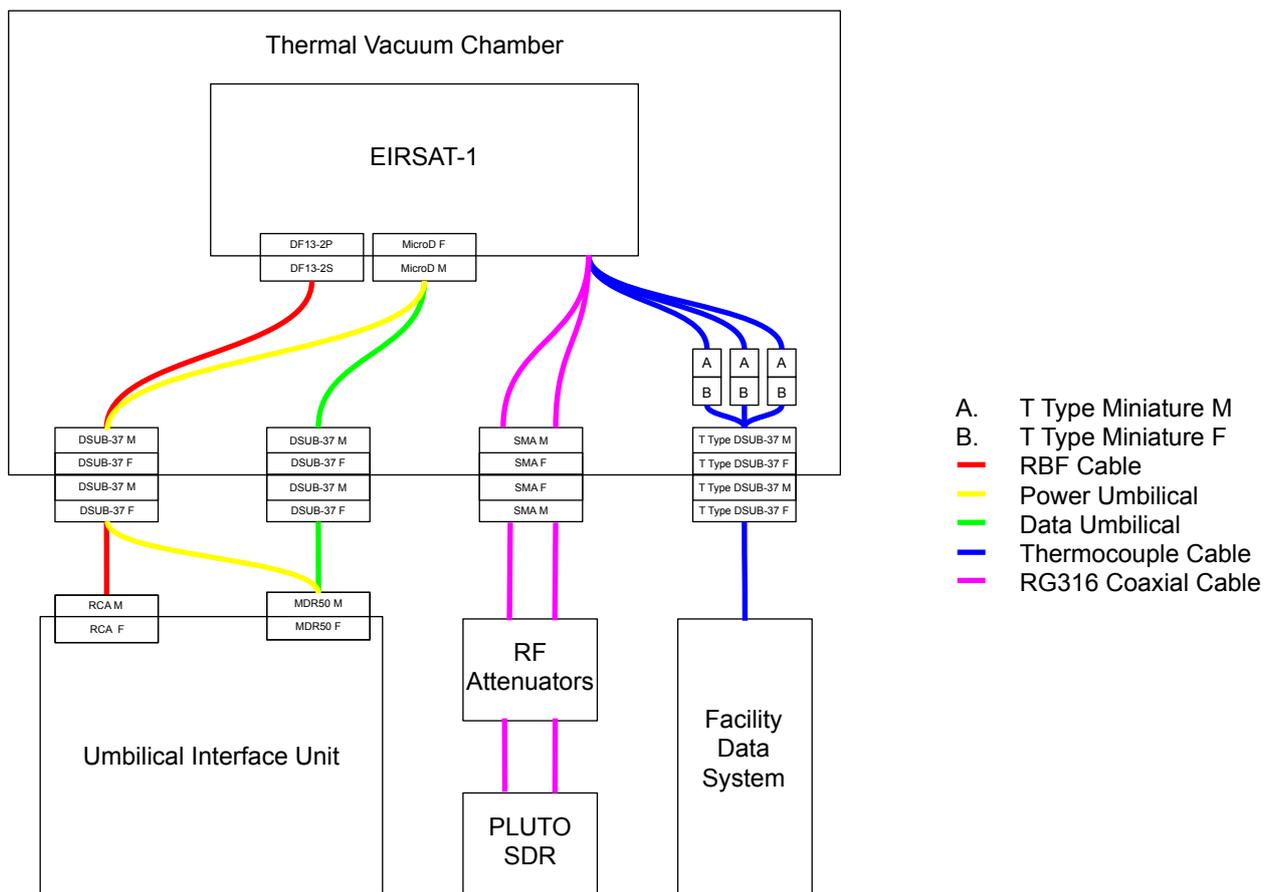
Figure 6. Schematic showing the end-to-end connections from the EIRSAT-1 spacecraft to the EGSE while integrated into the TVAC chamber.

The umbilical harness breaks into two separate D-SUB37 connectors, one for power and one for data. These were connected to the interior of the chamber flange. On the exterior of the chamber, the umbilical harness was connected to the in-house developed umbilical interface unit (UIU). The UIU allowed test operators to connect key pieces of test equipment to the spacecraft such as logic analysers for probing data lines, a power supply

for charging the battery, and a laptop running EIRSAT-1's mission control software for communication with the OBC when it was preferable to communicate with the satellite over serial rather than RF. The UIU also allowed operators to switch off the satellite using the RBF inhibit via a toggle switch. The UIU was connected to the EIRSAT-1 laptop that hosted the mission control software and displayed the debug log from the spacecraft. Grafana [54] was employed during testing for data visualisation, where real time and archived data could be monitored and reviewed. This web-based tool was useful in anomaly investigations and monitoring the temperature of the different subsystems over weekends.

4. EQM Thermal Test Campaign Results

The thermal testing and verification campaign of the EIRSAT-1 EQM took place from the 27 September 2021 to 14 October 2021. Over three weeks, the EIRSAT-1 EQM was subjected to one non-operational cycle, three and a half operational cycles, and one thermal balance test. The main sequence of events that occurred over the test campaign are summarised in Figure 7.
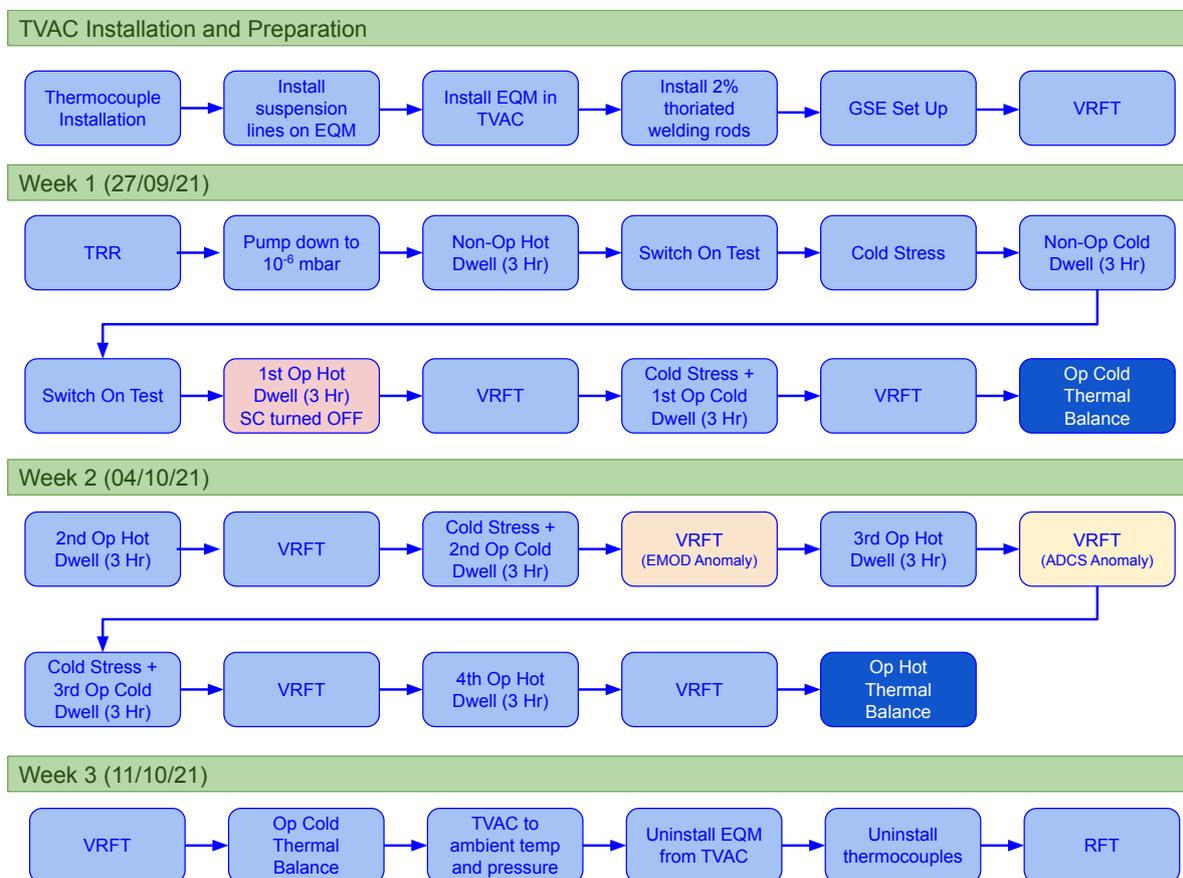
Figure 7. Main events and tests performed during the three week thermal test campaign with the EIRSAT-1 EQM at the ESA CSF. VRFTs where anomalies were observed which resulted in NCRs are highlighted in orange (EMOD) and yellow (ADCS). The operational hot cycle where the S/C had to be turned off to prevent battery temperature limits being exceeded is highlighted in red. The two TBal phases performed over weekends are depicted in dark blue.

The thermal profiles of the full campaign are presented in Figures 8–11. During the TBal hot phase, the facility computer rebooted resulting in a loss of some of the data as observed in all the thermal profiles. A deviation from the test plan was that the cold TBal profile was completed over the first weekend between operational cycles as discussed in Section 4.1.4. In Figure 8, the two temperature plateaus observed are due to the satellite

being in two different configurations. Two major but expected offsets can be observed in the profiles:

- The difference in temperature between the CSF sensors on the TVAC shroud and the TRP located on the external rail of EIRSAT-1.
- The offset between the sensors on the internal components and the external components of EIRSAT-1.

During the campaign, it was essential to have a sufficient understanding of these offsets to define suitable test levels to stress the spacecraft without exceeding any of the subsystem operational limits. The cold thermal balance phase led to a redefinition of the TRP temperature set points. For comparison with the test plan temperatures in Table 4, Table 7 presents the actual temperatures the EQM was cycled through during the test campaign. The definition of new test levels was driven by an advanced understanding of the internal dissipation of the spacecraft and the requirement to keep all components within their operational limits, the reasoning is discussed in more detail the following sections.

Table 7. Test campaign operational, non-operational, and thermal balance temperatures.

Test Level	Temperature (°C)	Tolerance (°C)	TRP Range (°C)
$T_{max, non-op}$	+56	−0/+4	+57 to +59
$T_{min, non-op}$	−16	−4/+0	−17 to −19
$T_{max, op}$	+28	−0/+4	+29 to +31
$T_{min, op}$	−6	−4/+0	−7 to −9
$T_{min, stress}$	−26	−4/+0	−27 to −29
$T_{max, TBal}$	+20	−0/+4	+21 to +23
$T_{min, TBal}$	−1	−4/+0	−2 to −4

Figure 8 displays the offset between the COTS components of EIRSAT-1, the TRP, and the sensors on the CSF TVAC. Additionally, the appearance of the thermal profile of the CMC is due to the temperature increasing every two minutes during transmission of the S/C beacon over RF. The sharp spikes of the light grey profile (T setpoint) are due to changes in the shroud set point. The profile of the sensors on the external components of the EQM is shown in Figure 9, which are as expected in close agreement to the TRP and BKTRP. To aid visualisation, the profile of the sensors on the ADM are displayed in Figure 10. As the ADM is on the −Z face of the S/C, its temperature profile is expected to be in close agreement with the TRP for the majority of the campaign. The deployment of the antenna with primary resistors and the primary and secondary resistor burn tests are expected to cause a rapid and large increase in temperature which can be seen as sharp peaks in the profile of ADM PCB sensor. Finally, the profile of the thermocouples installed on the GMOD and EMOD experiments and motherboards are displayed in Figure 11. As expected, given the design and desired performance of the EMOD thermal coupon assembly, it is well thermally isolated from the rest of the satellite. During the subsystem thermal test campaign of GMOD, it was observed that the scintillator acted as a heat sink, drawing heat via conduction from the rest of the instrument [39]. However, as there was no temperature sensor on the crystal during this testing, this effect can not be seen and it did not impact the thermal cycling of the system during this campaign.
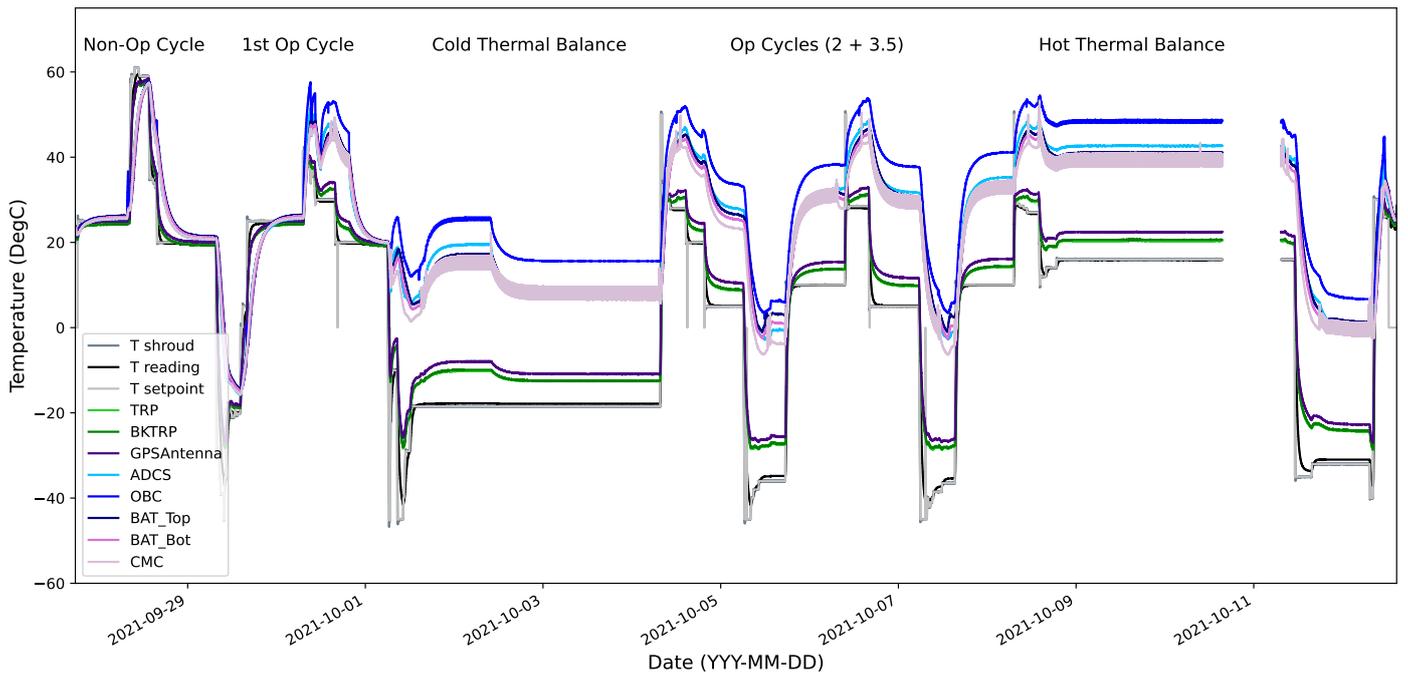
Figure 8. Thermal profile of COTS components and the CSF facility sensors with TRP and backup TRP for reference.
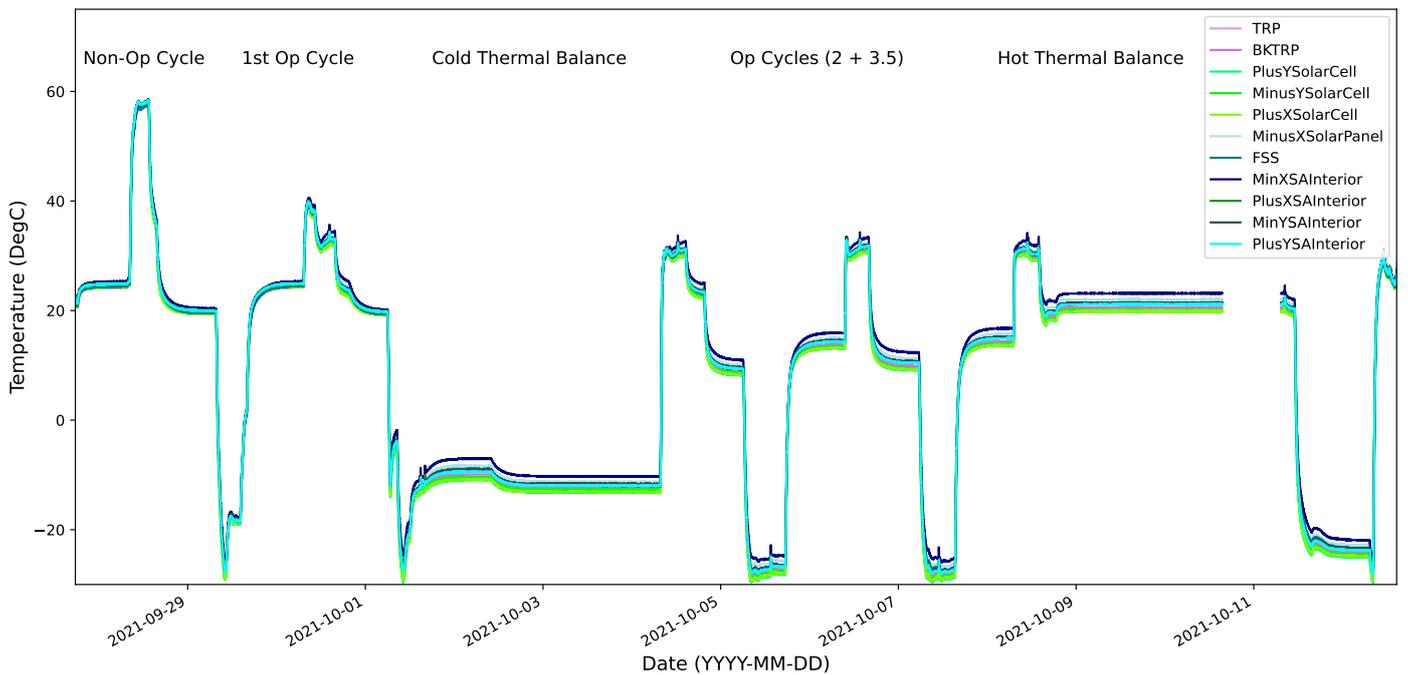

Figure 9. Thermal profile of sensors on external components of spacecraft with TRP and backup TRP for reference.
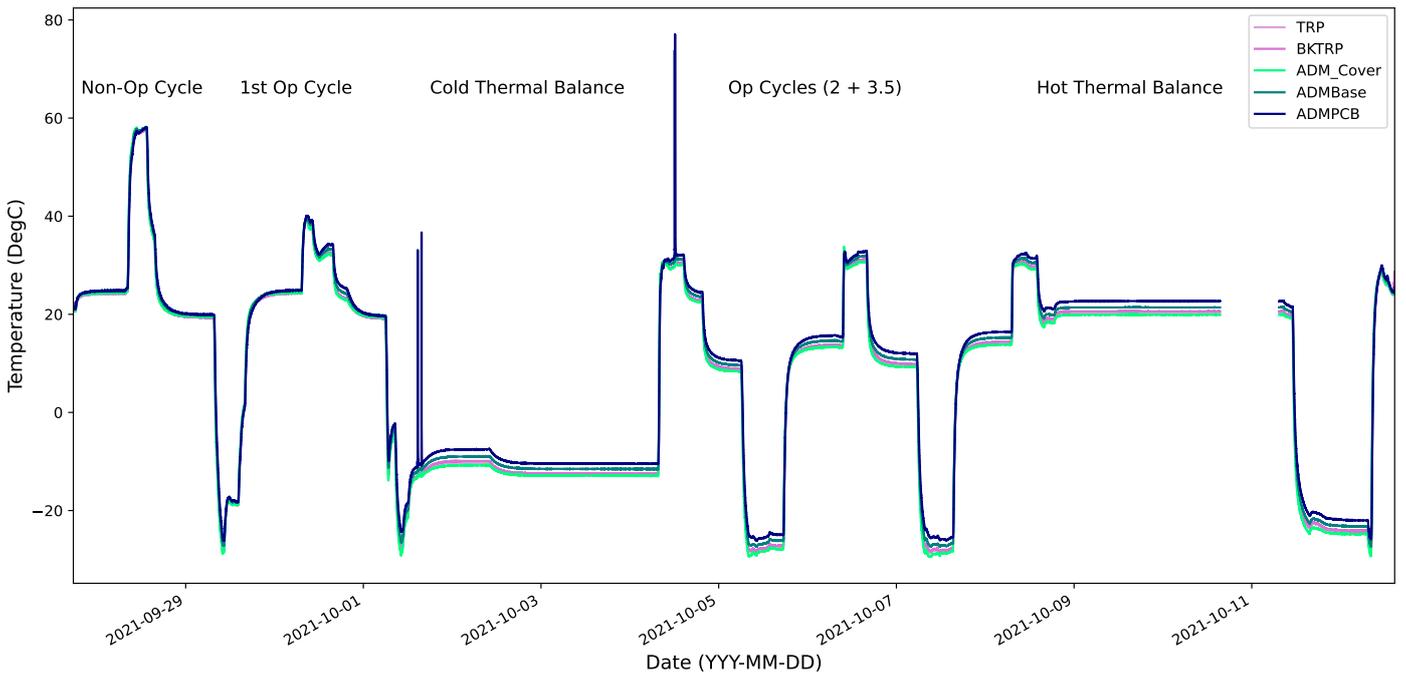
Figure 10. Thermal profile of ADM sensors where the deployment of the antenna and the primary and secondary resistor burn tests can be seen as sharp peaks in the temperature profile of ADM PCB sensor.
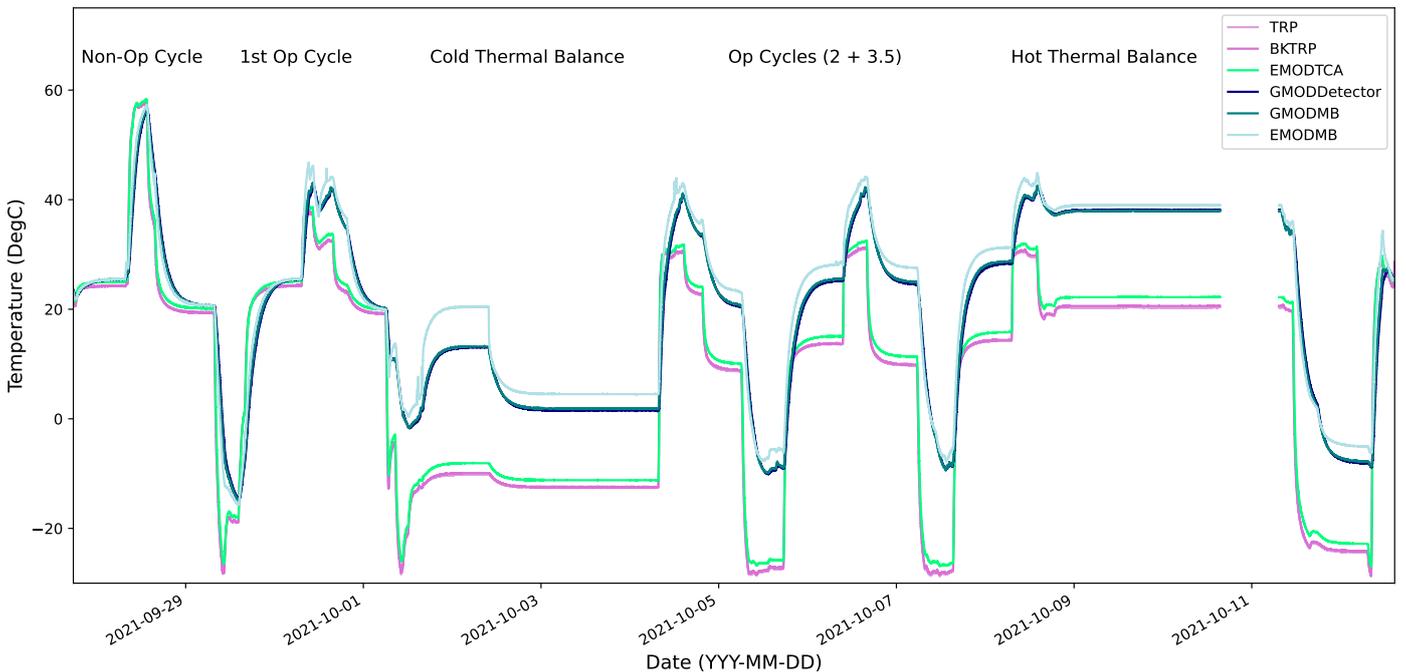
Figure 11. Thermal profile of sensors on payload (GMOD and EMOD) with TRP and backup TRP for reference.

4.1. Thermal Test Overview

Initially the external CSF thermocouples were installed by facility operators on the exterior of the S/C. EIRSAT-1 was then installed in the TVAC chamber as described in Section 3. The GSE external to the chamber which was used to communicate and operate the satellite while in the TVAC was assembled. The final activity performed before closing the chamber door was a VRFT, which confirmed that the GSE set-up was functional and the S/C could be operated while in the TVAC. Section 4.2 provides an overview of the results

from all the functional tests performed during this campaign. The EQM was then powered off and the TVAC was pumped down to $\sim 10^{-6}$ mbar.

4.1.1. Thermocouple Calibration Issue

It was observed before beginning any thermal cycling that there was an offset in temperature between the CSF sensors and the calibrated readings of the EIRSAT-1 temperature sensors installed in the EQM. Since the S/C was powered off overnight and should have no internal dissipation, it was expected that all the sensors would be in close agreement. It was important to have confidence in the output of the internal sensors on the different subsystems as these temperature readings were used to ensure that the components would never exceed their non-operational and operational limits. It was found that the raw sensor readings were in close agreement with the facility sensor readings. Prior to cycling it was agreed between the EIRSAT-1 team and the ESA CSF operators to use the non-calibrated values of the EIRSAT-1 temperature sensors, and instead increase the uncertainty on the readings to $\pm 1.5\,^{\circ}\mathrm{C}$. This was a conservative uncertainty based on the thermocouple data sheet with a theoretical uncertainty of $\pm 0.5\,^{\circ}\mathrm{C}$, plus a 1 degree uncertainty to account for the interface between the sensors and the DAQ.

4.1.2. Non-Operational Phases

Due to moving from the EIRSAT-1 calibrated sensor readings to the raw readings, it was noted that there was an issue with the definition of the TRP in the test specification. The defined range for the campaign, between $+57\,^{\circ}\mathrm{C}$ and $+59\,^{\circ}\mathrm{C}$ for the non-operational hot cycle could no longer be used, as with the new $\pm 1.5\,^{\circ}\mathrm{C}$ uncertainty, the battery temperature limit of $60\,^{\circ}\mathrm{C}$ could be exceeded. The rate of change of the battery was monitored for two hours with the TRP temperature range reduced to $[+54.5\,^{\circ}\mathrm{C}, +58.5\,^{\circ}\mathrm{C}]$. It was concluded the battery would not exceed its limits during the dwell and the TRP range was returned to $[+57\,^{\circ}\mathrm{C}, +59\,^{\circ}\mathrm{C}]$, with the caveat that the battery would not be allowed to exceed $+58.5\,^{\circ}\mathrm{C}$. During this first dwell at $\mathrm{T_{max,\,non-op}}$, it was observed that most subsystems would not reach their target temperatures, so the dwell time for this and all future dwells was increased to three hours. The chamber set point was then reduced and once all the subsystems were within their operational range, a switch on test was performed. The cold stress phase and non-operational cold dwell for three hours were completed as planned and the switch on test was performed once all subsystems were in their operational limits. All three battery heaters turned on during this test, confirming their functionality.

4.1.3. First Operational Phase

The charging of the S/C was switched on at a rate of $10\,\mathrm{W}$ during the ramp up to $\mathrm{T_{max,\,op}}$ ($36.5\,^{\circ}\mathrm{C}$) for the first operational cycle. Approximately one hour into the dwell, a rapid increase in the battery temperature was observed. The battery temperature could not exceed $48.5\,^{\circ}\mathrm{C}$, accounting for the battery operational limit of $50\,^{\circ}\mathrm{C}$ and the $1.5\,^{\circ}\mathrm{C}$ uncertainty. Charging was disabled when the battery temperature reached $48.2\,^{\circ}\mathrm{C}$; however, its temperature continued to increase. Once the battery reached its operational limit of $48.5\,^{\circ}\mathrm{C}$, a decision was rapidly made to power off the S/C via the RBF, to reduce the risk of damage to the subsystem. As the battery was off, it could reach $60\,^{\circ}\mathrm{C}$, its non-operational temperature limit. Once the battery had cooled sufficiently, the S/C was powered back on as the risk of damage was no longer a concern. The dwell was recommended but the battery reached its operational limits again and the S/C had to be powered off. The cause was presumed to be the significant power dissipation while charging of $\sim 10\,\mathrm{W}$. Due to these events, a new TRP target temperature was set at $30\,^{\circ}\mathrm{C}$, instead of the original $36.5\,^{\circ}\mathrm{C}$, and the charging profile for the campaign was reassessed. Only a trickle charging rate was allowed during the hot and cold dwells and during ramp down to cold temperatures to limit the impact of the S/C dissipation. A VRFT was performed successfully. Due to the S/C being powered off multiple times, it was decided to add a fourth hot operational phase after the three operational cycles were completed to fully qualify the EQM.

The chamber was set to start to cool overnight in preparation for the first cold operational cycle. However, during the night, the S/C powered off automatically due to low battery voltage, which triggered the battery's low voltage protection feature. Charging was not turned on overnight as there was no way to remotely turn off charging before ramping down to $T_{min, op}$. The automated cold cycle was stopped remotely to keep the battery above 0 °C. The S/C was charged at max rate for two hours until the battery was fully charged before the cold cycle was resumed.

4.1.4. Cold Thermal Balance Phase

The cold stress phase was performed and after a three hour dwell at $T_{min, op}$, a VRFT was completed. It was decided to transition to the cold TBal phase and complete it over the weekend instead of after all the operational cycles as proposed in the plan in Section 2.2. Performing the cold TBal over the weekend optimised the time available to the EQM in the CSF and provided an opportunity to advance the understanding of the dissipation of the subsystems in different satellite configurations e.g., specific payloads on/off, RF on/off, GPS on/off, different operational modes.

During the cold balance, the S/C was put into the following two configurations:

1.   S/C in nominal mode with GMOD and EMOD ON and in idle mode i.e., no experiment running. FSS was on, RF was enabled, and the ADCS Manager was enabled, meaning that the GPS was turned on for 2 min every 20 min. Charging was active and in end of charge mode.
2.   S/C in safe mode so all payloads are powered off, and ADCS Manager is off. RF was enabled. Charging was active and in end of charge mode.

It is evident from Figure 8, that once the payloads were off and the S/C in safe mode, an operational mode entered in case of an anomaly, where only critical subsystems are active, the internal dissipation decreased, and the S/C entered a second cold balance phase at a lower temperature over the second half of the weekend. The cold TBal criteria of 0.5 K/4 h were met successfully over the weekend and a VRFT was performed at the start of the second week.

4.1.5. Remaining Operational Phases

The cold thermal balance phase allowed for a redefinition of the TRP set points as the offset between the temperature of the external structure and the limiting subsystem, the battery, was better understood. For the remaining three operational hot phases the TRP range was set to [+29 °C, +31 °C]. The second and third cold stress and operational phases were performed as planned. As in Figure 3, there were anomalies observed during the VRFT after the second cold operational phase and the third hot operational phase. These will be discussed in detail in Section 4.2.

4.1.6. Hot Thermal Balance Phase and Post Test Review

After the extra fourth operational hot phase was performed and the VRFT completed, the test transitioned to a hot thermal balance phase over the second weekend of the test campaign. The S/C was in nominal mode with both GMOD and EMOD in their experiment modes. The FSS and ADCS Manager were on and RF was enabled. The TRP was set to +20 °C to account for the internal dissipation in the S/C; this is significantly lower than the proposed +31.5 °C in the test specification .

At the end of the thermal balance hot phase, it was noted that the facility computer that was recording the TVAC and thermocouple data rebooted resulting in a loss of data which can be seen in Figures 8–11. The facility software does not auto-save the thermocouple data. However, upon inspection of the data gathered until the last manual save of the data, it was verified that the hot stabilisation criterion had been met.

The first part of the PTR was performed to ensure the test objectives had been achieved before returning the chamber to ambient conditions. Once the chamber was vented to ambient pressure, the door was opened and a visual inspection of the EQM was performed.

It was observed that the ADM doors constraining the −X and +X elements had only partially opened following deployment. This was due to the kapton tape that was added to the coiled −X and +X elements to prevent full deployment (as mentioned in Section 3), which led to the coiled elements becoming jammed in the ADM rather than springing out and opening the doors. As the tape was only added to facilitate the test set-up, this issue does not cause reason for concern with respect to the actual on-orbit ADM performance. The EQM was removed from the TVAC chamber, the facility temperature sensors were removed from the exterior, and it was set up for the post TVAC RFT, with the results of this functional test detailed in Section 4.3. The three week campaign was concluded with the second half of the PTR.

4.2. VRFT Results

A total of nine VRFTs were performed during the EIRSAT-1 EQM thermal test campaign; this is one more than in the test specification due to the extra operational hot phase being performed. The content of the VRFTs was not the same throughout the campaign. The tests performed during each VRFT are detailed in Table 6 for the payload and COTS subsystems, and Table 8 displays the payloads tested in the different VRFTs.

Table 8. Functional tests performed with payloads (ADM, EMOD, and GMOD) during VRFTs and RFT. A tick indicates the test was included and a dash means the test was not performed.

Subsystem	ADM		EMOD		GMOD	
Test Activity	Primary deployment	Resistor burns	Payload power cycle	Read RTD measurements	Payload power cycle	Generate lightcurve and spectrum with a radioactive source
Ambient VRFT	—	—	—	—	✓	✓
Non-Op Hot Switch On Test	—	—	—	—	—	—
Non-Op Cold Switch On Test	—	—	—	—	—	—
Op Hot 1 VRFT	—	—	—	—	✓	✓
Op Cold 1 VRFT	✓	✓	—	—	✓	✓
Op Hot 2 VRFT	—	✓	✓	✓	✓	✓
Op Cold 2 VRFT	—	—	✓	✓	✓	✓
Op Hot 3 VRFT	—	—	✓	✓	✓	✓
Op Cold 3 VRFT	—	—	✓	✓	✓	✓
Op Hot 4 VRFT	—	—	✓	✓	✓	✓
Hot Thermal Balance VRFT	—	—	✓	✓	✓	✓
Post TVAC RFT	✓	✓	✓	✓	✓	✓

The ADM functional tests were not performed until the VRFT after the first operational cold cycle to verify successful deployment of the ADM in the cold case as the team has confidence of its performance in the hot case from subsystem testing [55]. The EMOD

motherboard will host the firmware for the ADM at launch, as the ADM PCB does not have a dedicated microcontroller. The EMOD MB will then be reprogrammed with EMOD firmware once the antenna have been successfully deployed. The EMOD functional tests were not included in the VRFTs until the second operational hot cycle after the ADM had been tested in both extreme hot and cold conditions and the EMOD MB had been flashed with the EMOD firmware.

The majority of the functional tests performed were automated to increase the efficiency, avoid the possibility of human error, and ensure the tests were being exactly replicated after each dwell. The automated test scripts, developed in Python, sent TCs to the S/C via the EIRSAT-1 mission control software on the EIRSAT-1 laptop and then verified the response received using the appropriate pass/fail criteria.

A deviation from the test plan was to create a 'Basic Health Check' form, which was filled out at the start and end of every day of testing to monitor the state of the S/C and know the expected state for each morning. The following parameters were recorded for the basic health check: operational mode, RF (ON/OFF), GMOD (ON/OFF), EMOD (ON/OFF), FSS (ON/OFF), and battery voltage. This record of the S/C configuration was extremely helpful when the S/C was in an unexpected state during the campaign.

GMOD displayed anomalous behaviour related to data generation during the RFT after the EQM vibration test campaign. While discussion of this anomaly is outside the scope of this paper, a deviation from the proposed functional test plan was required to allow the tests to continue. The automated script for setting up the GMOD experiment to record a spectrum and light curve was updated to allow a modified configuration to be uploaded to the ASIC on the GMOD motherboard. This configuration restored GMOD to normal operation by filtering out the new narrow peak that was observed post-vibration and did not further affect the TVAC campaign.

The majority of the functional tests in each VRFT were passed successfully; however, there were a number of anomalies encountered during the three weeks of testing. For severe anomalies that required further investigation, an NCR was issued. Table 9 presents the main anomalies encountered by the EIRSAT-1 team during the thermal test campaign. The remainder of this section will describe the anomalies encountered, the root cause and solution or the current status of the investigation.

Table 9. List of anomalies encountered during EQM thermal test campaign and the documentation required to record the anomaly occurrence and possible solution.

Anomaly	Documentation Required	Responsible
Battery Temperature Limit	Minor NCR	EIRSAT-1/ESA
EMOD Data Transmission	Major NCR	EIRSAT-1
ADCS Gyro Comms Error Flags	Major NCR	EIRSAT-1
CMC "Check 9" at low temperatures	Minor NCR	EIRSAT-1
Loss of data due to CSF computer crash	Minor NCR	ESA

4.2.1. Battery Temperature Limit Anomaly

As described in Section 4.1, during the first operational hot phase, the S/C had to be powered off twice during subsequent dwell attempts at $T_{max, op}$ to prevent the battery operational temperature limits being exceeded. The dissipation of the S/C while charging was higher than expected and led to the unexpected increase in the battery temperature. The CSF operators reduced the temperature of the TVAC environment to attempt to reduce the battery temperature without success. Once the battery reached its operational limit, the S/C was powered off to protect the batteries and ensure the test requirement of not exceeding any operational limits of the subsystems was not violated. After this anomaly was encountered, the TRP set points and charging profile of the EQM test campaign were revised to levels informed by the first TBal phase to prevent this anomaly from occurring again. A minor NCR was raised to describe the events and what actions can be taken

to prevent this occurring during the FM test campaign. A TBal phase will be performed at the beginning of the FM thermal test campaign to have a better understanding of the dissipation of the S/C before performing any thermal tests.

4.2.2. EMOD Data Transmission Anomaly

EMOD displayed anomalous behaviour during the functional test after the second cold operational cycle. It was first noted when the automated test script failed due to there being no increase in data being received by the OBC from EMOD. In the debug output, a "bad frame signature" error was observed. During this and subsequent VRFTs, this unexpected behaviour was investigated using a logic analyser. It was determined that the serial transmission of data from EMOD to the OBC was failing due to byte-level framing errors. EMOD makes use of its embedded processor's internal clock generator, which is based on an internal oscillator. The resonant frequency of this oscillator is temperature-dependent [56]. During the cold dwell, where the EMOD microcontroller was at $-5°$, it was found to be running approximately 1% slow, effectively leading to an EMOD-OBC baudrate mismatch. The errors raised in the debug output were due to the OBC incorrectly interpreting the transmitted data. The original EMOD firmware (v2.2.9) had a baudrate of 500 kbaud which was at the upper limit of what could be handled by the OBC. The solution proposed was to decrease the baudrate such that the OBC could better handle the bit-timing mismatches. A new firmware needed to be generated, as the baudrate is hardcoded, and flashed onto the EMOD MB while the EQM was still in the TVAC. It was found that using a lower baudrate restored EMOD experiment functionality. A new firmware (v2.2.10) with a baudrate of 125 kbaud enabled the OBC to reliably receive data from EMOD at lower temperatures. This new firmware will also run on the FM, as it has been confirmed to function in both high stress and ambient environments. A major NCR was raised for the EIRSAT-1 team to detail the EMOD anomaly events and lower baudrate solution.

4.2.3. ADCS Gyro Communications Anomaly

During the VRFT after the third hot operational cycle, it was observed that the Y gyro communications error flag was raised. The error flag appeared to have been raised during the reduced mode changes test. Upon inspection, a significant current peak in the 5 V bus was observed due to several subsystems being powered on at once such as when the S/C transitions from safe mode to nominal mode. The error flag was manually reset to zero and the VRFT continued as the error flag being raised seemed to have no effect on the functionality of the S/C. Previous data from the ADCS gyros were reviewed and it was found that this and the Z gyro communications flag were being raised throughout mission testing. As this was observed months prior to the ETC, the unexpected behaviour in the TVAC may be unrelated. This resulted in a major NCR, and the team are currently investigating the root cause of this error flag being raised and the impact this anomaly could have on the mission. Although this anomaly could have been found via other testing, it does show that issues can be missed and each campaign adds robustness.

4.2.4. CMC "Check 9" Anomaly

During the dwell after the second cold operational phase, a debug message stating "Check 9 Failed" was observed. This event was raised by the OBSW with the event description stating the CMC temperature was starting to get high; however, the temperature of the CMC was at ∼0 °C. The OBSW monitors the CMC temperature, with the upper and lower limits defined as 55 °C and 0 °C, respectively. The OBSW behaved as expected and raised an event when the CMC temperature exceeded this range but the event description provided incorrect information to the S/C operators. As the CMC had never been below 0 °C before, this issue with the software had never been observed. The team raised a minor NCR detailing how this software issue will be remedied for the flight model, where a new event will be raised when the CMC is below 0 °C, and the Check 9 event will only be raised when the CMC exceeds 55 °C.

4.3. Post TVAC RFT

The Post TVAC RFT was completed successfully over two days with the EQM located outside of the TVAC in ambient conditions. Some modifications were made to the functional tests based on the anomalies that had been encountered and investigated over the duration of the thermal test campaign:

- The GMOD functional test was completed with the modified automated script where the new configuration file for the ASIC registers was uploaded. With the new ASIC configuration, GMOD successfully passed its functional test and produced a spectrum and light curve.
- After the EMOD anomaly investigation , the EMOD functional test script was run twice, first with the original firmware (v2.2.9) on the EMOD MB and then again with the new firmware (v2.2.10). The EMOD experiment functional test was passed with both firmware versions in ambient conditions. The new firmware (v2.2.10) was left on the EMOD MB as this version performed reliably in both ambient and high stress environments.
- An additional ADCS test was performed in an attempt to recreate the gyro communications anomaly observed in the TVAC. A script was developed to instruct the ADCS MB to transition between different modes and check the gyro error flags after each transition to see if they had been raised. The error flags were not raised when the script was run and it was concluded that the anomaly investigation should continue in the cleanroom in UCD and the thermal test campaign could be closed out with a successful RFT.

5. Lessons Learned

As this was the first thermal test campaign prepared and executed by the EIRSAT-1 team, an extensive amount of knowledge and improved understanding of the satellite was achieved. Technical issues found in the system and solutions to them were investigated reducing risk to the mission. In encountering anomalous behaviour from the satellite, the team had the opportunity to find and implement solutions to recover the mission in a flight like scenario. As part of this educational experience, the lessons learned by the EIRSAT-1 team that would be most beneficial to other CubeSat missions are as follows:

- Objectives of Thermal Test Campaign: Initially, the team considered the main objective of the system-level thermal test to be stressing of the spacecraft by thermal cycling between hot and cold. However, in preparing and executing the test campaign, the lesson learned was that the thermal vacuum test is primarily a functional test of the system. The objective is to allow as many subsystems as possible to stabilise at their expected operational extremes of temperature, both hot and cold, so that functional tests may be carried out in these space representative conditions and any anomalous behaviour may be detected and investigated. For a CubeSat, this can be challenging as the test item is physically quite small and does not usually have many active heating or cooling mechanisms on board. Therefore, stabilising the external parts of the satellite at their operational extremes can be difficult while respecting the temperature limits of internal components. Typically the dwell temperatures are limited by the more temperature sensitive internal components. The limiting subsystem in the case of EIRSAT-1 was the battery.
- Importance of Thermal Modelling: A thermal analysis of EIRSAT-1 was used to help define the dwell temperatures and durations for the thermal test. Early during the operational cycles, it became clear that this model and the simulations carried out on the model did not accurately represent the conditions in the TVAC of the dissipation of the satellite in different modes of operation. Ultimately this led to a redefinition of the dwell temperatures early in the test and the battery temperature limit anomaly discussed in Section 4.2.1. The EIRSAT-1 thermal analysis focused mainly on a transient analysis of the satellite in orbit. While this is important for

finding the operational limits of different components, this test highlighted the equal importance of steady-state thermal analyses of the satellite while in different modes of dissipation. The steady state analyses are important both for the definition dwell temperatures during TVAC tests and for correlation with data collected in any thermal balance phases. Finally, the creation of such a high fidelity thermal model, capable of making accurate predictions would require a continuous effort throughout the life of the project. Therefore, thermal modelling should not be thought of as something that is required only at the early or design phases of a project but requires continuous updating as the design matures, the understanding of the system improves, and test data is available to correlate with the model.

- Addition of an Initial Operational Thermal Balance Phase in Future Tests: The resources and expertise required to carry out thermal modelling to the high fidelity described above are often not available to educational CubeSat teams. Ideally, the results of the TBal tests from this campaign will be used to refine the current thermal model of the S/C. In the case that time and resources do not support this, the following alternative approach has been suggested. For the EIRSAT-1 FM thermal test an initial thermal balance phase(s) at ambient temperature will be added to gather data on the temperature differences between subsystems and components with on-board dissipation. This data can then be used to adjust dwell temperatures before cycling.

- Battery Charging Profile: Linked to the above point, the charging profile was not well defined prior to the campaign. The rate of charging implemented at the beginning of the campaign introduced a non-negligible impact on the dissipation of the test item which contributed to reaching the battery temperature limits during cycling. For the FM campaign, a charging plan will be well defined for the duration of the test and a limit on the rate of charging will be implemented.

- Automated Test Scripts: The automated test scripts in Python were developed in the month before the thermal test campaign and proved to be beneficial. The VRFTs could be completed within two hours, confirming the functionality of all the subsystems in an efficient and replicable manner. The GMOD and EMOD anomalies were raised when the test scripts terminated early due to unexpected behaviour from the payloads. The FM FFT and ETC will make use of improved automated test scripts to streamline the testing process.

- Experiment Firmware Flashing: It was important in both anomaly investigations for EMOD and GMOD that the firmware on the experiment motherboard could be flashed via the OBC. A new firmware with a lower baudrate restored EMOD operations. The flashing of firmware to GMOD aided the understanding of the unusual behaviour of the experiment and that it was not related to the firmware. Without this capability, there would be no way to fix firmware during thermal testing without opening the chamber.

- Pass/Fail Criteria: During the PTR, the pass/fail criteria of the test campaign were reviewed before returning to ambient conditions to ensure all the objectives of the test campaign were achieved. An example of a poor pass/fail criteria is that all functional tests must be passed for the test campaign to be considered successful. It is inevitable that some anomalies will be encountered during these test campaigns, but it should not automatically result in the campaign not being considered successful. In writing the FM pass/fail criteria, the team will carefully consider the impact they will have on the formal evaluation of the success of the test campaign.

- Schedule: The three-week schedule for the thermal test campaign was optimistic and had no margin for anomaly investigations or the required increased dwell times. The entire environmental test campaign was scheduled to be four weeks, but an extra week was added on to investigate issues that arose during the vibration campaign. In the original plan, the TVAC was to be returned to ambient temperature over the weekend. To ensure the TBal phases could be performed, they had to be completed over the weekend. The test operators ended up spending long days in the cleanroom

in order to complete all the functional tests within the window the EIRSAT-1 project had booked at the CSF. For FM a schedule will be developed that includes margin for anomaly investigations.

- Pre-Travel Checklists: One of the cables required for the configuration of the satellite in the TVAC was not packed and introduced a small delay in commencing the thermal test campaign. While a checklist was made by the team prior to the test campaign, it was not strictly checked off while packing and preparing for travel. The FM checklist will be checked off and reviewed prior to travel to ensure nothing is forgotten.

The majority of the experience shared in the above lessons learned can be utilised by CubeSat teams to streamline their thermal testing campaigns. It is essential to understand the objectives of the test campaign being performed and to clearly state the pass/fail criteria while considering the impact these will have on the outcome of the campaign as a success/failure. CubeSat teams may lack the expertise to create and maintain an accurate thermal model of their spacecraft. To improve their understanding of their spacecraft, before commencing the thermal test, a thermal balance phase at ambient with the spacecraft in different configurations could be used to update the test levels based on the observed dissipation.

In addition to the technical lessons learned, the EIRSAT-1 team share some logistical lessons learned. Preparation and organisation are key aspects of a successful test campaign as thermal testing can span weeks, and anomalies are inevitable. The automation of functional tests was found to reduce the time required at the facility and improve test-retest reliability. A realistic schedule, with ample margin for investigating issues that arise, is essential to a successful campaign. Furthermore, CubeSat teams should not neglect the importance of a pre-travel checklist to ensure that all the equipment required is transported to the test facility.

6. Future Work

Following this thermal test campaign, the EIRSAT-1 team are required to submit the relevant NCRs and TRPT for FYS! review. The NCRs will require further investigations into the anomalies encountered during thermal testing, such as the ADCS gyro communication error, of which the root cause is still unknown. The environmental test campaign marked the end of the suite of test campaigns performed with the EIRSAT-1 EQM. A qualification review will be conducted with members of the EIRSAT-1 team and of the FYS! Programme where the ambient (FFT and MT) and environmental test campaigns will be reviewed to confirm that the design of EIRSAT-1 has been verified for spaceflight. The feedback and lessons learned from the EQM campaigns will be applied to the preparation of the assembly of FM and its ambient and environmental testing.

The EIRSAT-1 FM will be launched and operated by students in UCD, with scientific data from its three experiments contributing to the detection of GRBs (GMOD), performance analysis of ENBIO Ltd.'s thermal surface treatments (EMOD), and a first in-space test of a novel attitude control algorithm (WBC). The EIRSAT-1 project has provided a foundation of expertise and experience, which will lead to the development of future satellites with scientific objectives. Future CubeSats will likely be larger (3U or 6U) and have one main scientific objective to reduce the complexity of the mission leading to lower costs and faster delivery timescales.

The dissemination of the work required to perform a thermal test campaign of a complex CubeSat with both COTS and in-house developed components will benefit other educational space missions and provide a basis on which to plan and execute their own test campaigns.

7. Conclusions

Comprehensive system-level thermal testing is essential in qualifying the design of the spacecraft, determining its performance in a space representative environment, and reducing the risk of mission failure. Extensive preparation is required to execute a

successful thermal test campaign as demonstrated by the documentation required and in-depth considerations made in the determination of the test levels for the EIRSAT-1 EQM test campaign. The EQM remained functional after being subjected to one non-operational cycle, three and a half operational cycles, and a thermal balance test at the ESA CSF. The performance of the spacecraft was monitored via functional tests performed after dwelling at each temperature extreme. Anomalies were encountered such as the spacecraft needing to be powered off during the first hot operational dwell to protect the battery and the EMOD experiment not functioning at low temperatures. Without the thermal test campaign, the poor performance of EMOD would not have been revealed until flight. These challenges provided the opportunity to recover the mission and robustly test the ground station and functional test set-up capabilities of investigating anomalies with reduced access to the spacecraft. Moreover, four issues were uncovered which would not have been found in other tests and two more which had been previously missed. The campaign was a beneficial learning experience, highlighting the need for well-defined test levels based on an accurate thermal model, a thermal balance phase at the start of the campaign to understand the impact of the satellite's internal dissipation and the impact of the ability to reconfigure experiments on-orbit. The test campaign was ultimately successful and the expertise gained and lessons learned will be applied for the flight model test campaign and future missions.

Institutional Review Board Statement: Not applicable.

Informed Consent Statement: Not applicable.

Data Availability Statement: Data sharing is not applicable to this article.

Conflicts of Interest: The authors declare no conflict of interest. The funders had no role in the design of the study; in the collection, analyses, or interpretation of data; in the writing of the manuscript, or in the decision to publish the results.

Abbreviations

The following abbreviations are used in this manuscript:

ADCS	Attitude determination and control system
ADM	Antenna Deployment Module
ASIC	Application Specific Integrated Circuit
COTS	Commercial off-the-shelf
CSF	CubeSat Support Facility
DTMF	Dual-tone Multi-frequency
ECSS	European Cooperation for Space Standardisation
EGSE	Electrical ground support equipment
EIRSAT-1	Educational Irish Research Satellite
EMOD	Enbio Module
EPS	Electrical power supply
ESA	European Space Agency
EQM	Engineering qualification model
ETC	Environmental Test Campaign
FFT	Full Functional Test
FM	Flight model
FSS	Fine Sun Sensor
FYS!	Fly Your Satellite!
GMOD	Gamma-ray Module
GRB	Gamma-ray Burst
GSE	Ground Support Equipment
IUT	Item Under Test
LEO	Low Earth Orbit
MB	Motherboard
MGSE	Mechanical Ground Support Equipment
MT	Mission Test
MTQ	Magnetorquers
NCR	Non-Conformance Report
OBC	On-Board Computer
PCB	Printed Circuit Board
PTR	Post Test Review
RBF	Remove Before Flight
RF	Radio Frequency
RFT	Reduced Functional Test
RTD	Resistance Temperature Detector
S/C	Spacecraft
TBal	Thermal Balance
TC	Telecommand
TSpe	Test Specification
TRP	Temperature Reference Point
TRPT	Test Report
TRR	Test Readiness Review
TVAC	Thermal Vacuum
UCD	University College Dublin
UIU	Umbilical Interface Unit
VRFT	Very Reduced Functional Test
WBC	Wave Based Control

References

1. Heidt, H.; Puig-Suari, J.; Moore, A.; Nakasuka, S.; Twiggs, R. CubeSat: A New Generation of Picosatellite for Education and Industry Low-Cost Space Experimentation. In Proceedings of the 13th Annual AIAA/USU Small Satellite Conference, Logan, UT, USA, 23–26 August 1999 .
2. The CubeSat Program. *CubeSat Design Specification Rev. 14*; Technical Report CP-CDS-R14; California Polytechnic State University (Cal Poly): San Luis Obispo, CA, USA, 2020.
3. Nieto-Peroy, C.; Emami, M.R. CubeSat Mission: From Design to Operation. *Appl. Sci.* **2019**, *9*, 3110. [CrossRef]

4. Twiggs, R. Origin of CubeSat. In *Small Satellite: Past, Present and Future*; Helvajian, H., Janson, S.W., Eds.; The Aerospace Press: El Segundo, CA, USA, 2008; Chapter 5, pp. 151–173.

5. Swartwout, M. Reliving 24 Years in the next 12 Minutes: A Statistical and Personal History of University-Class Satellites. In Proceedings of the 32nd Annual AIAA/USU Small Satellite Conference, Logan, UT, USA, 4–9 August 2018.

6. Suhadis, N.M. Statistical Overview of CubeSat Mission. In Proceedings of the International Conference of Aerospace and Mechanical Engineering 2019, Penang, Malaysia, 20–21 November 2019; Rajendran, P., Mazlan, N.M., Rahman, A.A.A., Suhadis, N.M., Razak, N.A., Abidin, M.S.Z., Eds.; Springer: Singapore, 2020; pp. 563–573.

7. Kulu, E. Nanosatellite and CubeSat Database. Available online: https://www.nanosats.eu/database (accessed on 24 February 2021).

8. Serjeant, S.; Elvis, M.; Tinetti, G. The future of astronomy with small satellites. *Nat. Astron.* **2020**, *4*, 1031–1038. [CrossRef]

9. Liddle, J.; Holt, A.; Jason, S.J.; O'Donnell, K.A.; Stevens, E.J. Space science with CubeSats and nanosatellites. *Nat. Astron.* **2020**, *4*, 1026–1030. [CrossRef]

10. Deepak, R.A.; Twiggs, R.J. Thinking Outside the Box: Space Science beyond the CubeSat. *J. Small Satell.* **2012**, *1*, 3–6.

11. Mero, B.; Quillien, K.; McRobb, M.; Chesi, S.; Marshall, R.; Gow, A.; Clark, C.; Anciaux, M.; Cardoen, P.; Keyser, J.D.; et al. PICASSO: A State of the Art CubeSat. In Proceedings of the 29th Annual AIAA/USU Small Satellite Conference, Logan, UT, USA, 8–13 August 2015.

12. Straub, J.; Villela, T.; Costa, C.A.; Brandão, A.M.; Bueno, F.T.; Leonardi, R. Towards the Thousandth CubeSat: A Statistical Overview. *Int. J. Aerosp. Eng.* **2019**, *2019*, 5063145. [CrossRef]

13. Swartwout, M. The First One Hundred CubeSats: A Statistical Look. *J. Small Satell.* **2013**, *2*, 213–233.

14. Perumal, R.P.; Voos, H.; Dalla Vedova, F.; Moser, H. Small Satellite Reliability: A Decade in Review. In Proceedings of the AIAA/USU Conference on Small Satellites, Virtual, 7–12 August 2021.

15. Alanazi, A.; Straub, J. Engineering Methodology for Student-Driven CubeSats. *Aerospace* **2019**, *6*, 54. [CrossRef]

16. Monteiro, J.P.; Rocha, R.M.; Silva, A.; Afonso, R.; Ramos, N. Integration and Verification Approach of ISTSat-1 CubeSat. *Aerospace* **2019**, *6*, 131. [CrossRef]

17. Viquerat, A.; Schenk, M.; Lappas, V.; Sanders, B. Functional and Qualification Testing of the InflateSail Technology Demonstrator. In Proceedings of the 2nd AIAA Spacecraft Structures Conference (AIAA SciTech), Kissimmee, FL, USA, 5–9 January 2015; American Institute of Aeronautics and Astronautics Inc. (AIAA): Reston, VA, USA, 2015. [CrossRef]

18. Murphy, D.; Joe, F.; Thompson, J.W.; Doyle, M.; Erkal, J.; Gloster, A.; O'Toole, C.; Salmon, L.; Sherwin, D.; Walsh, S.; et al. EIRSAT-1—The Educational Irish Research Satellite. In Proceedings of the 2nd Symposium on Space Educational Activities, Budapest, Hungary, 11–13 April 2018; Bacsárdi, L., Ed.; Budapest University of Technology and Economics: Budapest, Hungary, 2018; pp. 201–205.

19. Vanreusel, J. Fly Your Satellite! The ESA Academy CubeSats programme. In Proceedings of the ITU Symposium & Workshop on Small Satellite Regulation and Communication Systems, Santiago de Chile, Chile, 7–9 November 2016.

20. Murphy, D.; Ulyanov, A.; McBreen, S.; Doyle, M.; Dunwoody, R.; Mangan, J.; Thompson, J.; Shortt, B.; Martin-Carrillo, A.; Hanlon, L. A compact instrument for gamma-ray burst detection on a Cubesat platform I: Design drivers and expected performance. *Exp. Astron.* **2021**, *52*, 59–84. [CrossRef]

21. Murphy, D.; Ulyanov, A.; McBreen, S. A compact instrument for gamma-ray burst detection on a Cubesat platform II: Detailed design, assembly and validation. *Exp. Astron.* 2021, *under review*.

22. Ulyanov, A.; Morris, O.; Hanlon, L.; McBreen, S.; Foley, S.; Roberts, O.J.; Tobin, I.; Murphy, D.; Wade, C.; Nelms, N.; et al. Performance of a monolithic LaBr$_3$:Ce crystal coupled to an array of silicon photomultipliers. *Nucl. Instrum. Methods Phys. Res. A* **2016**, *810*, 107–119. [CrossRef]

23. Ulyanov, A.; Morris, O.; Roberts, O.J.; Tobin, I.; Hanlon, L.; McBreen, S.; Murph, D.; Nelms, N.; Shortt, B. Localisation of gamma-ray interaction points in thick monolithic CeBr$_3$ and LaBr$_3$:Ce scintillators. *Nucl. Instrum. Methods Phys. Res. A* **2017**, *844*, 81–89. [CrossRef]

24. Mangan, J.; Murphy, D.; Dunwoody, R.; Doyle, M.; Ulyanov, A.; Hanlon, L.; Shortt, B.; McBreen, S.; Emam, M.; Erkal, J.; et al. Embedded Firmware Development for a Novel CubeSat Gamma-Ray Detector. *arXiv* 2021, arXiv:2111.03128.

25. Vedrenne, G.; Atteia, J.L. Gamma-Ray Bursts: The Brightest Explosions in the Universe. *Phys. Today* **2010**, *63*, 56.

26. On Semiconductor. *J-Series SiPM Sensors Datasheet—Revision 6*; Semiconductor Components Industries, LLC: Phoenix, AZ, USA, 2018.

27. Ulyanov, A.; Murphy, D.; Fredriksen, A.; Ackermann, J.; Meier, D.; Nelms, N.; Shortt, B.; McBreen, S.; Hanlon, L. Using the SIPHRA ASIC with an SiPM array and scintillators for gamma spectroscopy. In Proceedings of the 2017 IEEE Nuclear Science Symposium and Medical Imaging Conference (NSS/MIC), Atlanta, GA, USA, 21–28 October 2017; pp. 1–3.

28. Müller, D.; St. Cyr, O.C.; Zouganelis, I.; Gilbert, H.R.; Marsden, R.; Nieves-Chinchilla, T.; Antonucci, E.; Auchère, F.; Berghmans, D.; Horbury, T.S.; et al. The Solar Orbiter mission. *Astron. Astrophys.* **2020**, *642*, A1. [CrossRef]

29. O'Connor, W.; de la Flor, F.R.; McKeown, D.; Feliu, V. Wave-based control of non-linear flexible mechanical systems. *Nonlinear Dyn.* **2008**, *57*, 113–123. [CrossRef]

30. Sherwin, D.; Thompson, J.; McKeown, D.; O'Connor, W.; Sosa, V.U. Wave-based attitude control of EIRSAT-1, 2U cubesat. In Proceedings of the 2nd Symposium on Space Educational Activities, Budapest, Hungary, 11–13 April 2018; Bacsárdi, L., Ed.; Budapest University of Technology and Economics: Budapest, Hungary, 2018; pp. 273–277.

31. Thompson, J.; Murphy, D.; Erkal, J.; Flanagan, J.; Doyle, M.; Gloster, A.; O'Toole, C.; Salmon, L.; Sherwin, D., Walsh, S.; et al. Double dipole antenna deployment system for EIRSAT-1, 2U CubeSat. In Proceedings of the 2nd Symposium on Space Educational Activities, Budapest, Hungary, 11–13 April 2018; Bacsárdi, L., Ed.; Budapest University of Technology and Economics: Budapest, Hungary, 2018; pp. 221–225.

32. Doyle, M.; Gloster, A.; O'Toole, C.; Mangan, J.; Murphy, D.; Dunwoody, R.; Emam, M.; Erkal, J.; Flanaghan, J.; Fontanesi, G.; et al. Flight software development for the EIRSAT-1 mission. In Proceedings of the 3rd Symposium on Space Educational Activities, Leicester, UK, 16–18 September 2019.

33. Gamble, K.; Lightsey, G. Application of Risk Management to University CubeSat Missions. *J. Small Satell.* **2013**, *2*, 147–160.

34. Menchinelli, A.; Ingiosi, F.; Pamphili, L.; Marzioli, P.; Patriarca, R.; Costantino, F.; Piergentili, F. A Reliability Engineering Approach for Managing Risks in CubeSats. *Aerospace* **2018**, *5*, 121. [CrossRef]

35. Latachi, I.; Rachidi, T.; Karim, M.; Hanafi, A. Reusable and Reliable Flight-Control Software for a Fail-Safe and Cost-Efficient Cubesat Mission: Design and Implementation. *Aerospace* **2020**, *7*, 146. [CrossRef]

36. Walsh, S.; Murphy, D.; Doyle, M.; Reilly, J.; Thompson, J.; Dunwoody, R.; Erkal, J.; Finneran, G.; Fontanesi, G.; Mangan, J.; et al. Development of the EIRSAT-1 CubeSat through Functional Verification of the Engineering Qualification Model. *Aerospace* **2021**, *8*, 254. [CrossRef]

37. Walsh, S.; Murphy, D.; Doyle, M.; Thompson, J.; Dunwoody, R.; Emam, M.; Erkal, J.; Flanagan, J.; Fontanesi, G.; Gloster, A.; et al. Assembly, integration, and verification activities for a 2U CubeSat, EIRSAT-1. In Proceedings of the 3rd Symposium on Space Educational Activities, Leicester, UK, 16–18 September 2019.

38. Doyle, M.; Dunwoody, R.; Finneran, G.; Murphy, D.; Reilly, J.; Thompson, J.; Walsh, S.; Erkal, J.; Fontanesi, G.; Mangan, J.; et al. Mission testing for improved reliability of CubeSats. In Proceedings of the International Conference on Space Optics—ICSO 2020, Online, 30 March–2 April 2021; Cugny, B., Sodnik, Z., Karafolas, N., Eds.; International Society for Optics and Photonics, SPIE: Bellingham, WA, USA, 2021; Volume 11852, pp. 2717–2736.

39. Mangan, J.; Murphy, D.; Dunwoody, R.; Ulyanov, A.; Thompson, J.; Javaid, U.; O'Toole, C.; Doyle, M.; Emam, M.; Erkal, J.; et al. The environmental test campaign of GMOD: A novel gamma-ray detector. In Proceedings of the International Conference on Space Optics—ICSO 2020, Online, 30 March–2 April 2021; Cugny, B., Sodnik, Z., Karafolas, N., Eds.; International Society for Optics and Photonics, SPIE: Bellingham, WA, USA, 2021; Volume 11852, pp. 471–491. [CrossRef]

40. ECSS Secretariat. *Tailored ECSS Engineering Standards for In-Orbit Demonstration CubeSat Projects*; ECSS Standard; European Cooperation For Space Standardisation: Noordwijk, The Netherlands, 2016.

41. Bagagli, R.; Baldini, L.; Bellazzini, R.; Barbiellini, G.; Belli, F.; Borden, T.; Brez, A.; Brigida, M.; Caliandro, G.A.; Cecchi, C.; et al. Environmental tests of the flight GLAST LAT tracker towers. *Nucl. Instrum. Methods Phys. Res. Sect. A Accel. Spectrom. Detect. Assoc. Equip.* **2008**, *584*, 358–373. [CrossRef]

42. You, Z. Chapter 5—Ground Tests of Micro/Nano Satellites. In *Space Microsystems and Micro/Nano Satellites*; Micro and Nano Technologies; Butterworth-Heinemann: Oxford, UK, 2018; pp. 147–166. [CrossRef]

43. ESA Education CubeSat Support Facility. Available online: https://www.esa.int/Education/CubeSats_-_Fly_Your_Satellite/CubeSat_Support_Facility (accessed on 8 December 2021).

44. ECSS Secretariat. *ECSS Standard ECSS-E-ST-10-03C*; Space Engineering: Testing; European Cooperation For Space Standardisation: Noordwijk, The Netherlands, 2012.

45. Welch, J. Assessment of Thermal Balance Test Criteria Requirements on Test Objectives and Thermal Design. In Proceedings of the 46th International Conference on Environmental Systems, Vienna, Austria, 10–14 July 2016.

46. Obiols-Rabasa, G.; Corpino, S.; Mozzillo, R.; Stesina, F. Lessons learned of a systematic approach for the e-st@r-II CubeSat environmental test campaign. In Proceedings of the 66th IAC International Astronautical Congress, Jerusalem, Israel, 12–16 October 2015.

47. del Castillo-Sancho, C.; Grassi, G.; Kinnaird, A.; Mills, A.; Palma, D. Lessons Learned from AIV in ESA's Fly Your Satellite! Educational CubeSat Programme. In Proceedings of the AIAA/USU Conference on Small Satellites, Virtual, 7–12 August 2021

48. Fortescue, P.; Swinerd, G.; Stark, J. *Spacecraft Systems Engineering*, 4th ed.; Wiley: West Sussex, UK , 2011; Chapter 11.

49. Tribble, A. *The Space Environment: Implications for Spacecraft Design*; Princeton University Press: Princeton, NJ, USA, 1995.

50. Meseguer, J.; Pérez-Grande, I.; Sanz-Andrés, A. *Spacecraft Thermal Control*; Woodhead Publishing: Sawston, UK, 2012.

51. Complete CAD-based Thermal Engineering Tool Suite. Available online: https://www.crtech.com/products/thermal-desktop (accessed on 14 December 2021).

52. ECSS Secretariat. *ECSS Standard ECSS-E-ST-31C*; Thermal Control; European Cooperation For Space Standardisation: Noordwijk, The Netherlands, 2008.

53. Marshall, F.; Murphy, D.; Salmon, L.; O'Callaghan, D.; Doyle, M.; Reilly, J.; Dunwoody, R.; Erkal, J.; Finneran, G.; Fontanesi, G.; et al. Development of the Ground Segment Communication System for the EIRSAT-1 CubeSat. In Proceedings of the 16th International Conference of Space Operations 2021, Online, 3–5 May 2021; American Institute of Aeronautics and Astronautics: Reston, VA, USA, 2021.

54. Grafana Labs, Available online: https://grafana.com/ (accessed on 10 January 2022).

55. Thompson, J.; Reilly, J.; Murphy, D.; Salmon, L.; Doyle, M.; Dunwoody, R.; Rajagopalan Nair, R.; Erkal, J.; Finneran, G.; Mangan, J.; et al. Thermal Characterization Testing of a Robust and Reliable Thermal Knife HDRM (Hold Down and Release Mechanism) for CubeSat Deployables. In Proceedings of the 4th Symposium on Space Educational Activities, Barcelona, Spain, 27–29 April 2022.

56. Ibrahim, R.O.; Abd El-Azeem, S.; El-Ghanam, S.; Soliman, F. Studying the operation of MOSFET RC-phase shift oscillator under different environmental conditions. *Nucl. Eng. Technol.* **2020**, *52*, 1764–1770. [CrossRef]